Structural Damage Detection of Three-Dimensional Framed Structures via Experimental Measured Modal Parameters

By

Yuk Pan FUNG

Submitted in partial fulfillment of the requirements for
the degree of Bachelor of Engineering (Honours) in Building Engineering
(Structural and Geotechnical Engineering)

Department of Civil and Architectural Engineering
City University of Hong Kong

April 2014

Abstract

In recent years, the deterioration of aging bridges in Hong Kong has been the one of the major concerns in civil engineering. However, for most overpasses in Hong Kong, the damage detection method is still staying in visual inspection. It is necessary and urgent to develop advanced system for the maintenance purpose.

In this thesis, finite element model updating method would be introduced in damage detection of a scaled three-dimensional model. The methodology, testing procedures, modal identification and the analyzing processes would be discussed in the later chapters. By using two-step optimization approach, the duration of damage detection can be shortened compared to the traditional method, and it is very accurate which would be showed in the thesis later.

By applying the finite element model updating method mentioned in this thesis in real situation, the instant monitoring of the real infrastructures such as overpasses can be achieved. As a result, the cost for maintenance can be largely reduced due to the decrease of demand in human resources.

Acknowledgements

First of all, I would like to express my greatest appreciation and most sincere gratitude to my supervisor Dr. LAM, Heung Fai for giving me a opportunity to the final year project on model updating utilizing measured vibration. He is a helpful and insightful teacher who provides guidance and support for my final year project.

I would also like to thank Jia Hua YANG who is a Ph.D.student in City University of Hong Kong. He put a lot of effort in my final year project, and guiding me to achieve the success for this project.

In addition, I am also grateful to the technical staffs who were helping in developing the scaled model.

Finally, I would like to appreciate my girlfriend and my parents for their understanding when I’m writing this thesis. Thank you for all you done for me!

Table of Contents

Abstract 3

Acknowledgements 4

Table of Contents 5

List of Symbols 8

List of Figures 9

List of Tables 13

CHAPTER 1: INTRODUCTION ..... - 1 -

1.1 Background and Motivation ..... - 1 -

1.2 Objective and Scope ..... - 2 -

1.3 Organization of Thesis ..... - 2 -

CHAPTER 2: Literature Review on Vibration-Based Structural Health Monitoring ..... - 4 -

2.1 Overview of Past Research ..... - 4 -

2.2 Modal-based damage detection methods ..... - 6 -

2.2.1 Methods based on modal frequency ..... - 6 -

2.2.2 Methods based on changes in mode shape ..... - 7 -

2.2.3 Methods based on mode shape curvature ..... - 8 -

2.2.4 Methods based on dynamic flexibility ..... - 9 -

2.2.5 Methods based on frequency response function ..... - 10 -

2.2.6 Methods based on model updating ..... - 11 -

2.3 Chapter Conclusions ..... - 13 -

CHAPTER 3: METHODLOGY OF FINITE ELEMENT MODEL ..... - 14 -

3.1 General Procedure of Finite Element Model updating ..... - 14 -

3.2 Objective Function ..... - 15 -

3.2.1 Frequency Residual ..... - 16 -

3.2.2 Mode Shape Residuals ..... - 17 -

3.2.3 Weighting ..... - 18 -

3.3 Selection of Updating Parameters ..... - 19 -
3.4 Optimization Algorithm ..... - 20 -
3.5 Chapter Conclusions ..... - 22 -
CHAPTER4: VIBRATION MEASUREMENT ..... - 23 -
4.1 Description of Scaled Model ..... - 23 -
4.2 Description of Experiment Equipments ..... - 26 -
4.2.1 Applications and Considerations of Accelerometers ..... - 26 -
4.2.2 Layout of Accelerometers in Scaled Model ..... - 27 -
4.2.3 Data Acquisition System ..... - 33 -
4.3 Description of loading and damage ..... - 35 -
4.4 Experiment Procedure ..... - 36 -
4.5 Chapter Conclusions ..... - 40 -
CHAPTER5: MODAL IDENTIFICATION ..... - 41 -
5.1 Output-only Modal Identification Method ..... - 41 -
5.2 Extracting Data & Mode Identification ..... - 42 -
5.3 Combine of Mode Shapes ..... - 45 -
5.4 Mode Shape Normalization ..... - 46 -
5.5 Modal Assurance Criterion ..... - 46 -
5.6 Chapter Conclusions ..... - 47 -
CHAPTER 6: DAMAGE DETECTION OF THREE-DIMENSIONAL SCALED BEAM-BRIDGE FRAME ..... - 48 -
6.1 Simulated Finite Element Model ..... - 48 -
6.2 Damage Detecting by Model Updating ..... - 49 -
6.2.1 Objective Function ..... - 49 -
6.2.2 Updating Parameters ..... - 50 -
6.2.3 Weighting Factors ..... - 51 -
6.2.4 Optimization Algorithm ..... - 51 -

6.3 Model Updating and Damage Detection ..... - 52 -
6.3.1 Model Updating of Undamaged Model ..... - 53 -
6.3.2 Damage Detection ..... - 61 -
6.4 Further Study - Frequency Residual Only ..... - 73 -
6.5 Further Study – Discussion of Use of Optimization Method ..... - 74 -
6.6 Chapter Conclusions ..... - 74 -
CHAPTER 7: CONCLUSIONS ..... - 75 -
References ..... - 76 -
Appendix ..... - 80 -
Appendix A ..... - 80 -
Appendix B ..... - 91 -
Appendix C ..... - 98 -
Appendix D ..... - 99 -

List of Symbols

SHM	Structural Health Monitoring
VBDD	Vibration-Based Damage Detection
FRF	Frequency Response Function
MAC	Modal Assurance Criterion
COMAC	Coordinate Modal Assurance Criterion
DOF	Degree of Freedom
MSF	Modal Scale Factor

List of Figures

Figure 1.1 Classifications of Damage Detection Methods	5
Figure 3.1 General procedure of the Finite Element Model Updating method	15
Figure 4.1: Overview of model	24
Figure 4.2: Support condition of column	25
Figure 4.3: The scaled model and overpass in Hong Kong	25
Figure 4.4: Accelerometer	27
Figure 4.5: Theoretical vibration in x-direction	28
Figure 4.6: Theoretical vibration in y & z directions	29
Figure 4.7: Theoretical vibration in z-direction	29
Figure 4.8: Overview of finite element model	30
Figure 4.9: Placements of accelerometers	31-33
Figure 4.10: Analog Input Modules	34
Figure 4.11: Computer with LabView	34
Figure 4.12 Induced damage at node 6	36
Figure 4.13: Cross-section of beams	36
Figure 4.14 Measurement of set 1	37

Figure 4.15: Force on beams and column	38
Figure 4.16: Connection between accelerometers and recorders	39
Figure 4.17: Stabilization of accelerometers	39
Figure 5.1: Time domain data	43
Figure 5.2: Frequency Spectrum/Frequency domain data	43
Figure 6.1: Assignment of updating parameters	52
Figure 6.2: Joint Property	54
Figure 6.3: Frequency correlation of undamaged model	56
Figure 6.4: Mode shapes correlation of undamaged model	57
Figure 6.5: Comparison of experimental and theoretical vibration at mode 1 for undamaged model	57
Figure 6.6: Comparison of experimental and theoretical vibration at mode 2 for undamaged model	57
Figure 6.7: Comparison of experimental and theoretical vibration at mode 3 for undamaged model	58
Figure 6.8: Comparison of experimental and theoretical vibration at mode 4 for undamaged model	58
Figure 6.9: Comparison of experimental and theoretical vibration at mode 5 for undamaged mode	59
Figure 6.10: Comparison of experimental and theoretical vibration at mode 6 for undamaged model	59

Figure 6.11: Comparison of experimental and theoretical vibration at mode 7 for undamaged model	60
Figure 6.12: Comparison of experimental and theoretical vibration at mode 8 for undamaged model	60
Figure 6.13: Comparison of experimental and theoretical vibration at mode 9 for undamaged model	61
Figure 6.14: Comparison of experimental and theoretical vibration at mode 10 for undamaged model	61
Figure 6.15: Initial assignment of updating parameters for damaged model	63
Figure 6.16: Frequency correlation of damaged model	64
Figure 6.17: Mode shapes correlation of damaged model	65
Figure 6.18: Comparison of experimental and theoretical vibration at mode 1 for damaged model	65
Figure 6.19: Comparison of experimental and theoretical vibration at mode 2 for damaged model	66
Figure 6.20: Comparison of experimental and theoretical vibration at mode 3 for damaged model	66
Figure 6.21: Comparison of experimental and theoretical vibration at mode 4 for damaged model	67
Figure 6.22: Comparison of experimental and theoretical vibration at mode 5 for damaged model	67
Figure 6.23: Comparison of experimental and theoretical vibration at mode 6 for damaged model	68

Figure 6.24: Comparison of experimental and theoretical vibration at mode 7 for damaged model	68
Figure 6.25: Comparison of experimental and theoretical vibration at mode 8 for damaged model	69
Figure 6.26: Comparison of experimental and theoretical vibration at mode 9 for damaged model	69
Figure 6.27: Comparison of experimental and theoretical vibration at mode 10 for damaged model	70
Figure 6.28: Assignment of updating parameters for further damage detection	71
Figure 6.29: Frequency correlation of damaged model in further damage detection	72
Figure 6.30: Mode shapes correlation of damaged model for further damage detection	73

List of Tables

Table 5.1: Frequencies for each considered mode of undamaged model	44
Table 5.2: Frequencies for each considered mode for damaged model	44
Table 6.1: Results of updated parameters	54
Table 6.2: Comparison of experimental and theoretical modal properties of undamaged model	55
Table 6.3: Comparison of updated parameters between undamaged and damaged model	62
Table 6.4: Comparison of experimental and theoretical modal properties for damaged model	64
Table 6.5: Comparison of updated parameters between undamaged and damag model	70
Table 6.6: Comparison of updated parameters between undamaged and damaged model	71
Table 6.7: Comparison of experimental and theoretical modal properties of damaged model in further damage detection	72
Table 6.8: Comparison of updated parameters when using frequency residuals only	73

CHAPTER 1: INTRODUCTION

1.1 Background and Motivation

Deterioration is one of the major issues in civil structures such as highways, bridges and so on. As time goes by, fatigue failure would be developed due to repetitive traffic loads and the influences of environmental condition such as the difference in temperature, flooding and wind erosion. Maintenance is then required to improve the life-time and performance of civil structures especially for the ageing infrastructures.

According to the data from Highways Department, there are over 2000 overpasses in Hong Kong, and most of them built over thirty years ago. Therefore, the department conducts much regular maintenance to preserve the performance of bridge, which is usually in visual inspection. However the current method has some drawbacks. It cannot detect internal damage of a structural element, and may miss out damage developed during the gap of two inspections. Moreover, it is a time consuming and costly method, Highways Department spends over 7 million dollars per year and around 450 engineers in monitoring the structural health of overpass (Highways Department, 2009).

Due to the disadvantages of recent inspection methods, a promising method, called Structural Health Monitoring (SHM) has been introduced to increase the efficiency of infrastructure maintenance. In the theory of Structural Health Monitoring, the changes of structural properties such as mass and stiffness would affect the response of the structure. As a result, it is possible to utilize the

measured response in an inverse problem to recognize some unknown structural properties such as Young's modulus. Therefore, damage in infrastructures can be checked immediately, and it can reduce the requirement in human resources.

1.2 Objective and Scope

The current project aims to present and develop a finite element model updating approach that can used in damage detection on infrastructures such as overpass in Hong Kong. The overpass was simulated by a three-dimensional scaled beam-bridge frame model, and finite element model updating method was carried out to detect and localize the damage by utilizing ambient or free vibration. The methodology was reviewed in this thesis, and similar approach was then developed and applied in the three-dimensional model. All required procedures in vibration testing, modal identification and optimization were presented so that to generate the general flow path of damage detection. Finally, a two-step approach was used in damage detection which aims to improve the accuracy of damage localization and increase the time efficiency.

1.3 Organization of Thesis

The dissertation is organized in seven chapters.

Chapter 2 reviews the histories of modal-based damage detection method to show the state of art of damage detection.

Chapter 3 introduces the methodology of finite element model updating, and the main components such as objective function, selection of updating parameters and optimization algorithm would be described briefly.

Chapter 4 demonstrates the vibration experiment generally. The information of model, used equipments, damage description and testing procedures would be

presented to explain the flow path and requirements of testing.

Chapter 5 presents the modal identification technique in obtaining useful information from the raw data. The common data analyzing approaches such as mode shape normalization and modal assurance criterion would be demonstrated. And the difficulty in combining different sets of data to form a whole mode shape is overcome in this chapter.

Chapter 6 deals with the finite element model updating. It purposes to use the frequency and mode shape residuals to form the objective function. The selection of updating parameters and optimization algorithm is investigated. A two-step damage detection method would be introduced and compared with the original proposed method. Further study of objective function with frequency residuals only would be presented to see whether it can detect the damage location or not. In addition, some approaches in optimization are suggested to improve the efficiency.

Chapter 7 concludes the whole thesis and some recommendations are made.

CHAPTER 2: Literature Review on Vibration-Based Structural Health Monitoring

2.1 Overview of Past Research

The principle of Vibration-Based Structural Health Monitoring is based on the studying of the variation of response of the structure, so that the structural properties such as stiffness and mass can then be estimated. Vibration-Based damage detection is a proper technique to determine the damage properties of a structure such as location and extent utilizing structural response.

Vibration-Based Damage Detection (VBDD) can be divided into two steps: modal identification and damage detection. The first step modal identification is to calculate the modal parameters of a structure utilizing the measured time-domain data such as acceleration. Natural frequency, mode shape and damping are the common used modal parameters which can be used to characterize the response of a structure. Normally, the measurement of acceleration time data can be done by using accelerometers during the vibration of a structure. Then acceleration data can then be transformed into a frequency spectrum by using Fourier-Series or Fourier-Transform. Jean-Baptiste Joseph Fourier (1807) issued the use of Fourier-Series in heat transfer, and it can be applied in the representation of the frequency spectrum for period time series. The Fourier-Transform is also a mathematical transformation to represent the frequency spectrum for non-periodic time series. However, due to the time consumption and calculation complexity of Fourier-Transform, Fast Fourier-Transform (FFT) was developed to break down

the composite size of discrete Fourier-Transform into a smaller size for faster calculation (Cooley and Tukey, 1965). As a result, in practice, it is usually to use FFT to transform the measured structural response into frequency domain data. There is a massive study have been introduced to identify which modal parameters are sensitive to the changes of structural properties (Doebling et al.,1996, 1998; Sohn et al., 2003).

The second step damage detection is the correlation of the changes of modal parameters to the structural properties. In this stage, modal parameters would be used to identify the current performance of the structure. Recently, damage detection is classified into four levels:

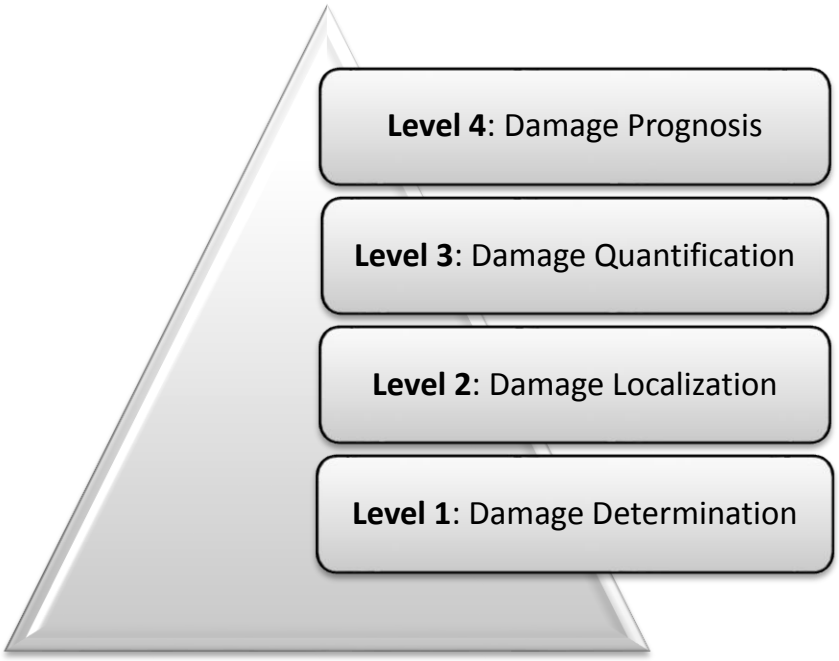

Figure 1.1 Classifications of Damage Detection Methods

At the level of determination, the present of damage can be recognized but the place of damage is unknown. The location of the damage can be identified in the level of localization. Most methods currently attain the level of quantification, which means they can detect the existence of damage, localize the damage, and

determine the extent of damage. And the level of damage prognosis, which is to predict the potential damage, is the current objective for SHM.

2.2 Modal-based damage detection methods

In general, damage detection methods can be divided into three areas, time domain, frequency domain and time-frequency domain. For the time domain methods, some of them are using minimum rank perturbation theory for damage detection (Kaouk and Zimmerman, 1992). There is also a study using moment as damage indicator (Zhang et al., 2013). For the time-frequency domain methods, they are based on some analysis techniques such as Hilbert-Huang Transform (Huang et al., 1998; Xu and Chen, 2004) and Wavelet Transform (Hou and Noori, 1999). The major vibration detection methods nowadays are based on frequency domain which is using natural frequency, mode shape, mode shape curvature, dynamic flexibility, frequency response function and modal strain energy.

2.2.1 Methods based on modal frequency

Modal frequency is the most basic modal parameters used in damage detection as it can be measured using only few sensors. Around thirty-five years before, Cawley and Adams (1979) used modal frequencies in damage localization, but only single damage location was considered in their study. Their approach was later developed by Friswell et al. (1994). Besides, Stubbs and Osegueda (1990) used a method that is similar to the approach of Cawley and Adams (1979) for solving the inverse problem of damage localization. In their study, an error function was defined based on the difference of measured and theoretical modal frequencies. And then, they determined the location that can minimize the error function as the damage location.

However, modal frequency sometimes is not very sensitive to the damage location when there are only few frequencies used. Salawu (1997) reviewed the use of changes in natural frequency for damage detection, and the results show that it is difficult to localize damage when only changes in the modal frequency were utilized. There is another research, damage detection in offshore oil industry (Idichandy and Ganapathy, 1990), which shows that only the use of modal frequency is not enough for accurate damage detection. In the research, many cracks were simulated but natural frequencies changed obviously only for half of them, so they conclude that the modal frequency is not enough to localize all damages. It is better using modal frequency and other parameters together to improve the accuracy of damage detection.

2.2.2 Methods based on changes in mode shape

Mayes (1992) developed a damage detection method based on changes in mode shape. The principle of this process is to check the translational and rotational error of the mode shape between the finite element model and the tested structure. Based on this result, it is possible to localize damage. The skill mentioned above is similar to Modal Assurance Criterion (MAC) and Coordinate Modal Assurance Criterion (COMAC), which are the currently used methods. These two indicators usually expressed as

$$\mathrm{MAC}[\Phi_{ti}\,,\ \Phi_{ei}] = \frac{\left|(\Phi_{ti})^{T}(\Phi_{ei})\right|^{2}}{[(\Phi_{ti})^{T}(\Phi_{ti})][(\Phi_{ei})^{T}(\Phi_{ei})]} \tag{2.1}$$

where Φ_{ti} and Φ_{ei} are the theoretical and experimental mode shapes respectively.

$$\mathrm{COMAC}[\Phi_{ti}\,,\ \Phi_{ei}] = \frac{\sum_{i=1}^{N}|(\Phi_{ti})(\Phi_{ei})^{*}|^{2}}{[\sum_{i=1}^{N}(\Phi_{ti})^{2}][\sum_{i=1}^{N}(\Phi_{ei})^{2}]} \quad (2.2)$$

where N is the number of DOF, and * indicates the complex conjugate.

These two methods are using least-squares approach, which means the compared mode shapes are correlated when the outcome close to 1. Besides, MAC is not accurate when the frequencies between two modes are too close (Tshilidzi Marwala, 2010).

2.2.3 Methods based on mode shape curvature

Besides the using of modal frequency and mode shape as damage indicators, some researchers have been seeking a more sensitive modal parameter for damage detection. Model updating based on modal curvature is one of the examples, which is based on the relationship between the curvature and the stiffness of beam cross section. Pandey et al. (1991) utilize the difference of the modal curvature between undamaged and damaged condition to find out its damage location. The modal curvature values are extracted from mode shape utilizing central difference method. However, the result shows that there is not only a significant change in damage position but also some smaller changes in various undamaged locations. To solve the problem, Abdel Wahab and De Roeck (1999) suggested a curvature damage factor which is the average of the difference of curvature for all modes. When applied in the real situation, they found that the modal curvature of higher mode is not accurate enough, and the accuracy would be lower when there are more cracks.

Later on, Maeck and De Roeck (2003) introduced a method to estimate the structural stiffness based on direct stiffness calculation. The theory of this method is based on the following equation:

$$M = EI\frac{d^2x}{dy^2} \tag{2.3}$$

where EI is the flexural stiffness of the beam. By calculating the bending moment and shear force, and utilizing some mathematical operations, the flexural stiffness can then be calculated directly.

2.2.4 Methods based on dynamic flexibility

Apart from the curvature method, the use of dynamic flexibility matrices is another mode shape based method. The modal flexibility matrix can be written as following:

$$[f] = [\Phi][M]^{-1}[\Phi]^T = \sum_{i=1}^{n} \frac{1}{\omega_i^2}(\phi_i)(\phi_i)^T \tag{2.4}$$

where [f] is the flexibility matrix, [Φ] is the mass normalized mode shape matrix, [M] = $diag(\omega_i^2)$, and ω_i is the circular frequencies. From the above equation, it seems that mode shape value does not contribute to the flexibility matrix too much when the circular frequency is too large. As a result, the flexibility matrix can be determined more accurately at a lower circular frequency (Xu and Xia, 2012).

Pandey and Biswas (1994) introduced that the damage can be detected and localized by using the variations in the dynamic flexibility matrix. The flexibility matrix was directly calculated from a few of vibration, and a model was used to prove the used method. They used the proposed method to locate the damage of a beam under controlled testing environment. Finally, they concluded that it is difficult to locate the damage around the support of the beam, and it is very realistic in the real situation. For the further develop of this method, Bernal and Gunes (2002, 2004) combined the variations of

dynamic flexibility matrix into the damage locating vector for the damage localization.

Compared with different modal parameters such as natural frequency and mode shape, modal flexibility matrix has higher ability to indicate damage when only one type of modal parameters is used (Zhao and DeWolf, 1999).

2.2.5 Methods based on frequency response function

Samman et al. (1991) observed the variations in FRF signals of a scaled bridge model due to the damage present. The curvature values of FRF in wave form are used to determine the cracks in the model. Later, Lew (1995) presented a unique method for the localization of damage based on the contrast of the transfer function parameters between undamaged and damaged stages. Besides, Wang et al. (1997) also presented a novel damage detection algorithm by using the theoretical model and FRF obtained from two stages undamaged and damaged. In the numerical study, this method detected the location and extent of damage accurately even though there are 5% measurement errors.

According to the research of Sampaio et al., (1999), the FRF curvature method is well in determining, locating and quantifying the damage compared with mode shape curvature method and damage index method. In their study, the FRF curvature method utilizes only the measured data without the necessity for any modal identification.

2.2.6 Methods based on model updating

Finite element model updating is also one of the damage detection methods. The principle of this method is updating the design parameters of a finite element model by minimizing the difference of experimental and theoretical modal parameters. Basically, the objective function can be expressed as following equation:

$$\min J(\theta) = r(\theta)^T r(\theta) = \sum_{i=1}^{N} [r_i(\theta)]^2 \quad (2.5)$$

where $r(\theta)$ is the residual vector including the differences between theoretical and experimental modal parameters.

Different constraints and numerical scheme would be implemented in the optimization algorithm to solve non-linear least squares problems. In general, the residual vector would be adjusted to minimize the objective function so that the changes in design parameters can be estimated. Moreover, since different modal parameters affect the structural properties in different ratio, weighting factors can then be assigned to obtain higher accuracy. The weighting factors can be usually obtained from the standard deviation of the corresponding experimental modal parameters.

Different from the direct methods, damage detection based on the model updating is an iterative method. Even though many iterations and heavy computation are required in this method, the symmetry, positivity and sparseness in stiffness and mass matrices can be preserved. Furthermore, since the updated stiffness and mass matrices have more physical meaning, the changes in modal parameters can then be related.

Mottershead and Friswell (1993) provided a general review and description of finite element model updating method. Liu (1995) used experimental modal frequency and mode shape for damage detection in a simple supported beam. The optimization algorithm is based the minimization of error in modal eigenequation. And the measurement errors in the experiment were accounted by using perturbation analysis. Afterwards, Cobb and Liebst (1997) investigated damage detection method with Assigned Partial Eigenstructure approach. The required stiffness changes for the correlation between experimental and theoretical model are then determined. Then, the location and extent of damage could be estimated.

Xia et al. (2002) presented a method to detect damage utilizing the differences of modal frequencies and mode shapes before and after the damage. A steel cantilever beam and frame were used in the research, and data was collected under laboratory condition. The mean and standard deviation of the stiffness parameters of damaged model were calculated by using the perturbation method and Monte Carlo simulation. The results showed that the damage can be detected correctly when the probability of damage presence is high.

There is a comparative study presented by Jaishi and Ren (2005), which is studying influence of different residual parameters used in the objective function such as frequency, mode shape and modal flexibility. In this study, different combinations of residuals were used, and the result is that the objective function combined with all three residuals is the best for finite element model updating.

2.3 Chapter Conclusions

Most of the common damage detection methods are briefly reviewed in this chapter. In addition, it is helpful in the selection of damage detection method. Since the results of finite element model updating method are more meaningful in physical, it would be used in this project. Moreover, the finite element approach is more general in different structures as it is not necessary to generate specific matrix or function for one structure. This method can be applied in real infrastructures such as bridges by just modifying the geometric information to form a new finite element model. Therefore, finite element model updating method is selected in this project.

CHAPTER 3: METHODLOGY OF FINITE ELEMENT MODEL

In this chapter, the general procedure of finite element model updating in this thesis will be presented initially. After that, the main components of the optimization process will also be discussed, including formulated residuals, objective function, selection of updating parameters and optimization algorithm.

3.1 General Procedure of Finite Element Model updating

A vibration test is carried out, and the responses are recorded by accelerometers at different nodes. The measured data is then be analyzed and converted into useful modal parameters such as natural frequency and mode shape for model updating process. Simultaneously the finite element model is developed based on the initial trial values of unknown design parameters such as Young's modulus. Objective function is then defined based on the selected residuals and constraints, and optimization process would be proceeded to obtain best design parameters that fitting the theoretical and experimental model. The general procedure of the finite element model updating is shown in Figure 3.1.

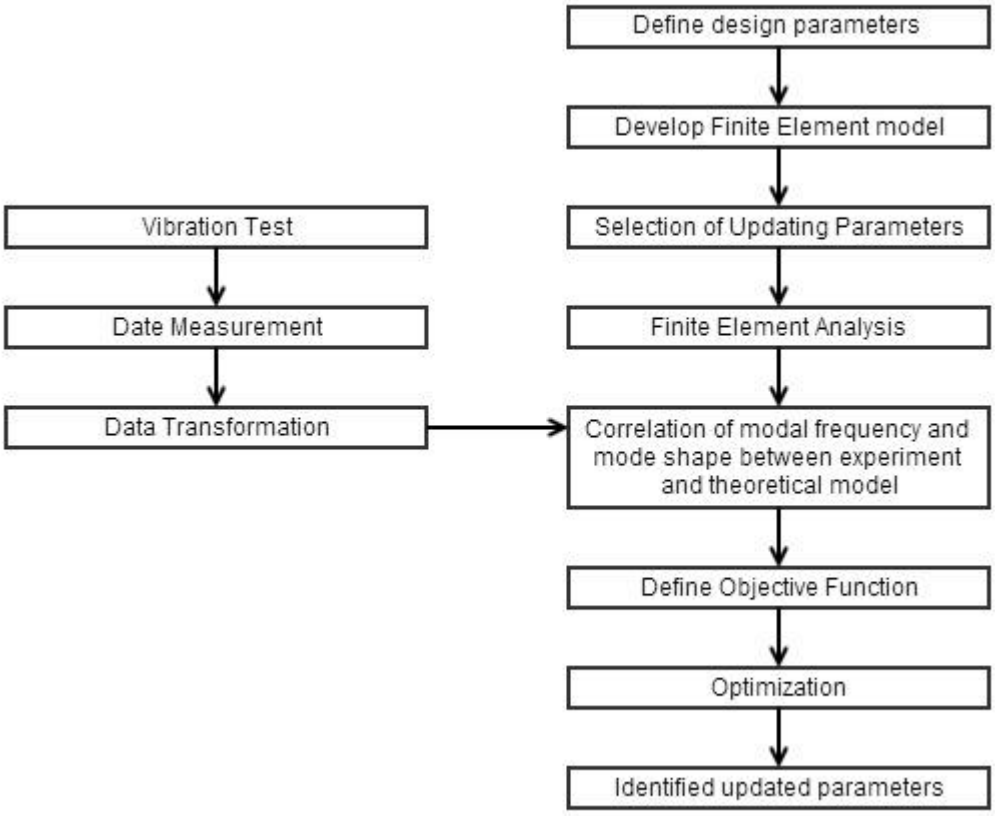

Figure 3.1 General procedure of the Finite Element Model Updating method

3.2 Objective Function

There are three main problems that impede the direct correlation between theoretical and experimental parameters. First, due to the current limitation of identification techniques, usually only some modes can be identified in experiment data. Second, the measurement locations are always less than that of the theoretical model. Third, there are some degree of freedom (DOF) can't be measured by today's techniques such as rotational DOF. Therefore, model reduction or data expansion always required, and it is time consuming. However, the above issues can be ignored when least squares approach is applied. It is because this approach does not need to compare all the modes, and only portion of modes are enough for accurate estimation.

The Least Squares approach is one of the general concepts that can be used in the defining of the objective function. As shown in the study of Mottershead et al. (2000), the objective function reflects the difference between the theoretical and experimental modal parameters of the structure. It usually can be represented as a sum of squared differences:

$$\min J(\theta) = \sum_{i=1}^{N}[z_i(\theta) - \bar{z}_i(\theta)]^2 = \sum_{i=1}^{N}[r_i(\theta)]^2 \quad (3.1)$$

where $z_i(\theta)$ represents the theoretical modal parameters and $\bar{z}_i(\theta)$ represents the experimental modal parameters. $r(\theta)$ is the residual vector including the differences between theoretical and experimental modal parameters. Equation (3.1) is the basic least squares function, but there are some advanced forms exist. For instance, residuals can be multiplied with a weighting factor in the objective function, so that the relative importance of different residuals can be considered separately.

3.2.1 Frequency Residual

The difference between the theoretical and experimental eigenfrequency is the most common and important residual for finite element model updating. This frequency can be solved from the eigenproblem, $\lambda = (2\pi f)^2$. The eigenfrequency residual can be express as:

$$r(f) = \sum_{i=1}^{N} \frac{f_{ti} - f_{ei}}{f_{ei}} \quad (3.2)$$

where the parameters f_{ti} and f_{ei} refer to the theoretical and experimental eigenfrequencies respectively. And the value N refers to the amount of selected eigenfrequencies that would be used in updating process.

The eigenfrequency can be measured and identified accurately from vibration experiment, and it provides global information of the structure. Therefore, it is usually used in finite element model updating. However, it is difficult to measure high natural frequencies and only changes in modal frequency are not enough for model updating (Salawu, 1997). Hence, another residual such as model shape is necessary to improve the objective function.

3.2.2 Mode Shape Residuals

Apart from frequency residual, mode shape residual is also introduced in the objective function in this thesis. The reason for utilizing mode shape differences for finite element model updating is that it contains spatial information about the structural dynamic behavior.

Before the correlation of theoretical and experimental mode shape, it should be normalized as the properties difference between theoretical and experiment model may cause a large error during optimization. There is no standard requirement of normalization of mode shape, but some approaches are commonly used recently. Allemang & Brown (1982) suggested that multiplying the experimental mode shape with a modal scale factor (MSF) so that the theoretical and experimental modal vectors can be scaled similarly. The equation of MSF is showed below

$$\mathrm{MSF} = \frac{\phi_{ti}{}^{T}\phi_{ti}}{\phi_{ei}{}^{T}\phi_{ei}} \tag{3.3}$$

Therefore, the mode shape residual can be expressed as (Friswell and Mottershead, 1995):

$$r(\phi) = \phi_{ti} - MSF \times \phi_{ei} \tag{3.4}$$

where ϕ_{ti} and ϕ_{ei} are the theoretical and experimental mode shape respectively.

Furthermore, the mode shape can also be normalized by using one reference node. In this approach, both theoretical and experimental mode shapes are normalized to one in the reference node which is usually the mode shape with the largest amplitude.

After many trials of expression, Moller and Friberg (1998) proposed to use the following equation as mode shape residual.

$$r_i^2(\phi) = \frac{\left(1-\sqrt{MAC_i}\right)^2}{MAC_i} \tag{3.5}$$

where MAC is defined in Equation (2.1).

3.2.3 Weighting

In the objective function, different types of residual can be weighted differently according to their importance and measurement accuracy. Since eigenfrequency residual and mode shape residual would be used in objective function in this thesis, the formulated objective function is:

$$\min J = \sum_{i=1}^{N}\left(\omega_f\left|\frac{f_{ti}-f_{ei}}{f_{ei}}\right|\right) + \sum_{i=1}^{N}(\omega_m|1-MAC|) \tag{3.6}$$

where the first part is the eigenfrequency residual, and the second part is the mode shape residual. ω_f and ω_m are the weighting factors of eigenfrequency and mode shape respectively. In general, compared with measurement of

mode shape, natural frequency can be measured more accurately with present technology. According to Friswell and Mottershead (1995), the percentage error of measured natural frequencies within 1% and that of mode shape within 10%. Thus, higher weighting factor can be applied in to the eigenfrequency residual.

3.3 Selection of Updating Parameters

The selection of updating parameters is crucial in the success of model updating. The updated model will not have any physical meaning if the updating parameters are wrongly selected. Material properties and geometrical properties are commonly used as updating parameters. Since geometrical properties can be measured very accurately in the selected scaled model in this experiment, only material properties such as Young's modulus, moment of inertia, etc. are considered in this thesis. The selection of updating parameters in this thesis will be further discussed in Chapter 6.

In addition, the number of updating parameters is also a main concern. The number of potentially varied parameters may be huge. However, it is impossible to update all parameters as most of them are not erroneous, otherwise the updated model would become physically unreasonable. To prevent ill-conditioned problem, the number of selected parameters should be as less as possible.

To reduce the numbers of updating parameter, a grouping approach can be implemented. The updating parameters can be selected in elemental level or substructure level. For example, all nodes in one structural element can be grouped, and they share the same updating parameter. Then the mass and stiffness

matrix can be written as:

$$\Delta K = \sum_{i=1}^{N} a_i K_i \tag{3.7}$$

$$\Delta M = \sum_{i=1}^{N} b_i M_i \tag{3.8}$$

where K_i and M_i are the stiffness and mass matrices of i-th elements or substructure respectively. The values a_i and b_i are the updating parameters. The error would be indicated if a_i or b_i larger or smaller than one, otherwise the structural elements are healthy if a_i and b_i equal to one.

3.4 Optimization Algorithm

The objective function can be minimized by using optimization algorithms. Optimization methods can be classified into linear and non-linear. It can be also classified into constrained and unconstrained, and the constraints can be dived into equality and inequality one. The general optimization problem can be expressed as:

$$\begin{aligned} &\min J(x) \\ \text{subject to} \quad &C_i(x) = 0\,, \\ &C_i(x) \le 0\,, \\ &\text{low}(x) \le x \le \text{up}(x) \end{aligned} \tag{3.9}$$

where $J(x)$ is the objective function. $C_i(x)$ is a vector function that contains equality and inequality constraints. x is the vector of coefficient of design parameters, which is constrained by lower bound and upper bound. The optimization algorithm would proceed many iterations to find out the optimized solution. Initially, a guess of vector of design parameters x would be assigned into the objective function. Afterward, iterations of vector x would be proceeded until the optimal solution is attained.

To take one case as an example, objective function with only eigenvalues λ is used. The example objective function is showed below:

$$\min J = \sum_{i=1}^{N}[\lambda_{ti}(x) - \lambda_{ei}]^2 = [\lambda_{ti}(x) - \lambda_{ei}]^T[\lambda_{ti}(x) - \lambda_{ei}] \qquad (3.10)$$

The minimum J can be achieved when its gradient equal to zero. By differentiating the objective function with respect to the coefficient of design parameter x, the derivate is:

$$\frac{\partial J}{\partial x} = 2S^T[\lambda_{ti}(x) - \lambda_{ei}] \qquad (3.11)$$

where the matrix S is the sensitive matrix of eigenvalues with respect to x. By using Nelson's method (Nelson, 1976), the sensitive matrix can be calculated.

For the constrained optimization problem, it can be also solved by active-set method. The theory of active-set method is dividing the constraints into active and inactive parts. When the constraint is equal to zero at bounded feasible region, it is called active. Otherwise, if the constraint is not equal to zero at bounded feasible region, it is called inactive. To explain, take a constraint from equation (3.9) as example

$$C_i(x) \leq 0 ,$$

For every x values inside the bounded area $low(x) \leq x \leq up(x)$, the constraints can be equal to zero or smaller than zero. Therefore, active and inactive set can then be divided. During iterations, the coefficient of design parameters x would be dived into two groups, fixed and free variables. The optimization problem can be mitigated when using active-set method as there are some coefficients of design parameters x can be defined as free variables without constraints. As a result, the size of the problem can then be reduced. However, both active and inactive set are required to be updated at each iteration, it slowdown the process of optimization.

Optimization can be done by using computer program such as MATLAB nowadays. There is several optimization algorithms can be selected in MATLAB depending on the objective function, gradient and constraints.

3.5 Chapter Conclusions

This chapter reviews the general requirement in using the finite element model updating method. The main components such as objective function, updating parameters and optimization algorithm are clearly discussed. It provides a guide to develop own finite element model in this project.

CHAPTER4: VIBRATION MEASUREMENT

This chapter will describe the geometric information of the scaled model first. Afterwards, the equipments used for measurement and data transmission will be introduced. Moreover, it also goes through the placement of measuring equipments, description of induced damage and the experiment procedures.

4.1Description of Scaled Model

The scaled model used for the experiment is a beam-bridge steel frame. It consists of two longitudinal beams, three transverse beams and six columns as showed in Figure 4.1. The width, height and length of the scaled model are 0.3m, 0.3m and 1.8m from center to center respectively. All structural elements used are rectangular in cross section. The cross sectional width and depth of each steel element are 0.5 inch and 1.2 inches (around 0.0127m and 0.03048m) respectively. The scaled model was built in two continuous spans and was supported by six columns. The bottom end of each column is welded into a square plate which is screwed into the ground floor (Figure 4.2). The thickness and size of the plate is calculated to resist rotation is the bottom end, and the square design is to prevent rotation in both x and y directions. In addition, four bolts are screwed deeply into the ground to ensure the moment can be transferred to the ground. As a result, the scaled model is in fix-support condition.

The shape and elements arrangement of the scaled model is designed as similar as overpass in Hong Kong (Figure 4.3). And the design of scaled model was based on scaled down design loading in real bridge design, which means the model can

support scaled deck and scaled vehicles without failure in beam deflection, compression, buckling and so on. There are two reasons will cause differences in modal parameters between the model and real bridge. The first one is the differences in Young's modulus between steel and reinforced concrete. And the second one is the ignored mass from deck and vehicles. However, the concepts and procedures of model updating are similar. Therefore, this scaled model is used for model updating in this thesis.

Figure 4.1: Overview of model

Figure 4.2: Support condition of column

Figure 4.3: The scaled model and overpass in Hong Kong

4.2 Description of Experiment Equipments

4.2.1 Applications and Considerations of Accelerometers

In this experiment, accelerometers were used to measure the acceleration data from each node. It was because the vibration measured in term of the acceleration can be more accurate than that of velocity, displacement and so on. In structural health monitoring, accelerometers are broadly used to measure induced vibration due to the impact or ambient force. In addition, the acceleration data is relatively highly related to the functionality and serviceability of civil structure such as bridge, and the modal parameters such as the natural frequency, mode shape and damping ratio can be easily transformed from the acceleration data. Therefore, accelerometers were selected as the measurement equipments in this experiment.

The selection of accelerometers is based on its sensitivity. It should be considered that piezoelectric type accelerometer may not be able to measure very low frequency response (near 0 Hz). It is a critical issue if this accelerometer is applied in the measurement of real civil infrastructure as the natural frequencies for some structures are very low. It is suggested to use piezoresistive type and capacitive type accelerometers in the real situation.

Ceramic Shear Accelerometers with Integrated Electronic Piezoelectric Output were used for measurement (Figure 4.4). These sensors can measure frequency within 0.5 Hz to 7000Hz, which is enough for this project, but it should be changed for real infrastructure measurement.

Moreover, the installation of accelerometers should be carefully considered.

The accelerometer would receive electric signals with respect to the acceleration of the base. Therefore, the accuracy of measurement highly depends on the orientation of accelerometers. From Figure 4.4, there is an arrow that specifies the required measurement direction, frequent and careful checks based on this arrow were carried out through the experiment.

Figure 4.4: Accelerometer

4.2.2 Layout of Accelerometers in Scaled Model

The number and placement of accelerometers should be depended on the required accuracy in the finite element model. It is well known that the more the divided elements, the higher the accuracy in a finite element model. However, due to the high cost of accelerometers, it is almost impossible to install many accelerometers in practice. There are two ways that can minimize the number of required accelerometers without losing too much important information.

First, the number of nodes required can be estimated from the mode shape of simulated model. From the simulated model, the vibration directions within 500Hz natural frequency are in both x, y and z direction, Examples were extracted from the simulated model and showed in Figure 4.5, Figure 4.6 and Figure 4.7 respectively. To obtain higher accuracy in model updating, three accelerometers were used to measure the responses in x, y and z direction of each node. In addition, by considering the deflection characteristics of each element, columns and transverse beams are always in single curvature, and the longitudinal beams are sometimes in single, double or even triple curvature. Therefore, three segments were divided into columns and transverse beams, and nine segments were divided in longitudinal beams. The divided segments and the total number of nodes are showed in Figure 4.8.

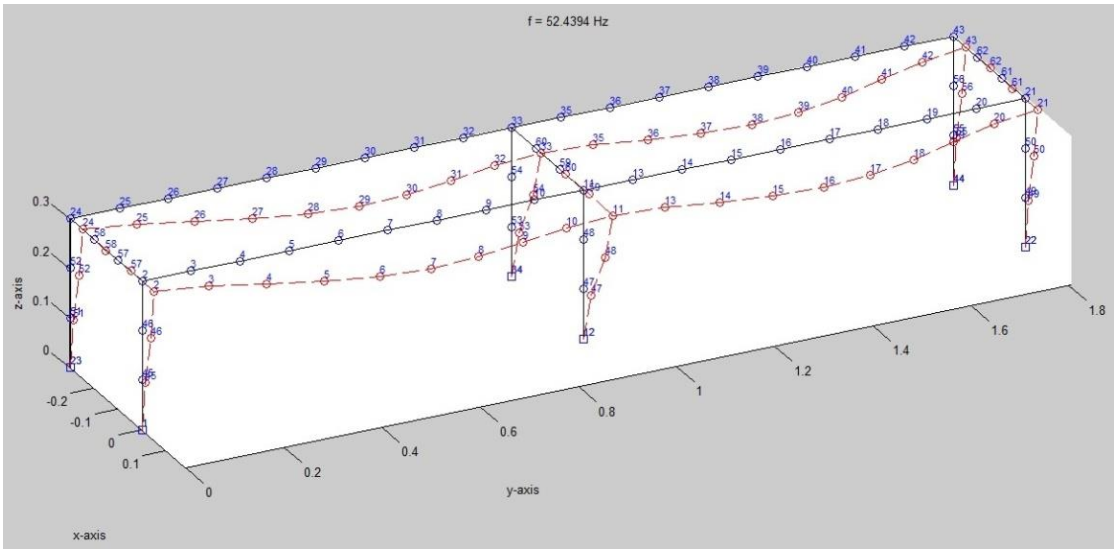

Figure 4.5: Theoretical vibration in x-direction

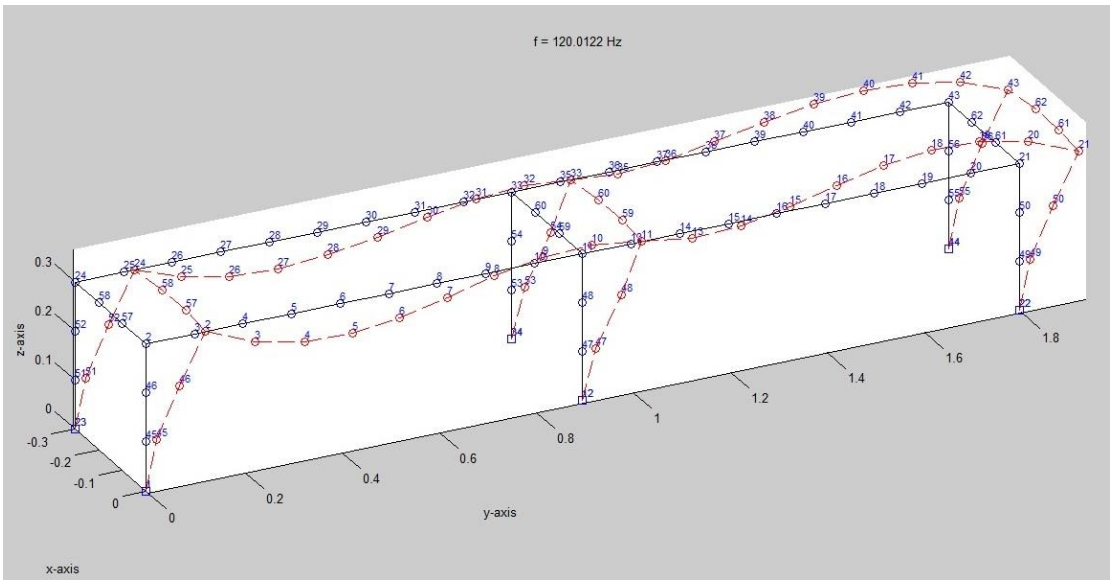

Figure 4.6: Theoretical vibration in y & z directions

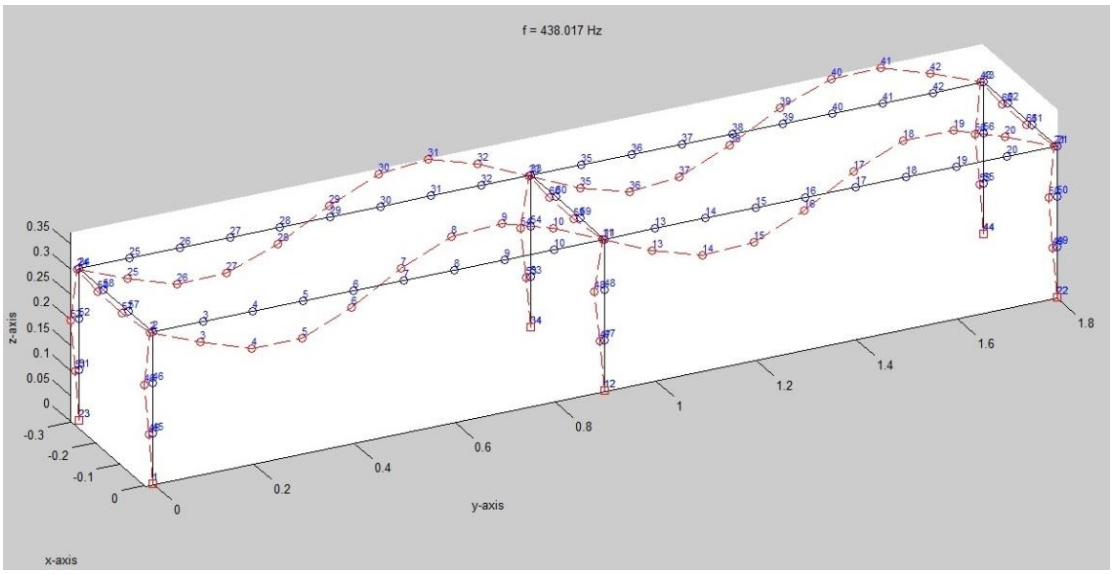

Figure 4.7: Theoretical vibration in z-direction

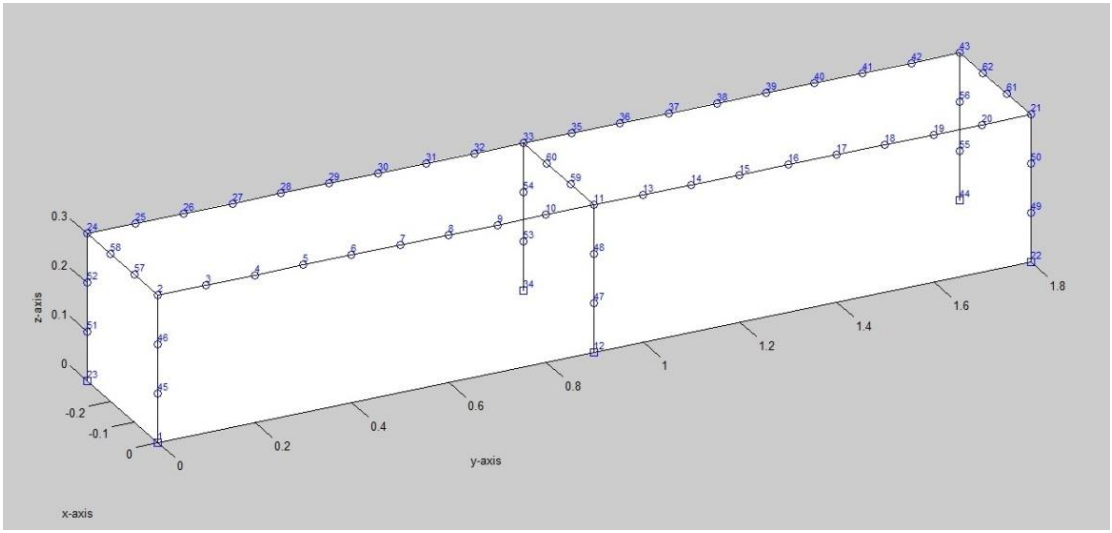

Figure 4.8: Overview of finite element model

Second, it is not necessary to measure the responses of all nodes simultaneously. Instead, the measurement was carried out in several sets to measure the response group by group. All required is only one or more reference points in each set of data for the combination of data. Different from the general procedure, the reference point was not always setting on one point only throughout the entire test. However, there is at least one common reference point between any two groups of measurement so the mode shape can be assembled (Au, 2011). From Figure 4.8, there are total 62 nodes but six of them (1, 12, 22, 23, 34 and 44) are fixed. And other nodes can vibrate and rotate in three directions, so there are totally three 336 DOF in the simulated model. However, the rotational DOF cannot be measured with current technology, and most translational DOF are not able to measure due to the design, except for node 2, 11, 21, 24, 33 and 43. For instance, it is almost impossible to measure the DOF of node six in y-direction. Therefore, the number of measurable DOFs is 118. Due to the insufficient of accelerometers, the measurement was divided into nine groups, and the locations of

accelerometers in each group are showed in Figure 4.9. The overlapped positions are the reference points between each group.

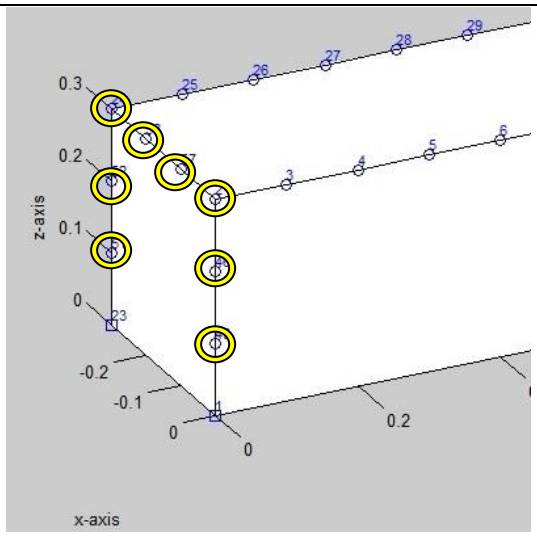

Set 1

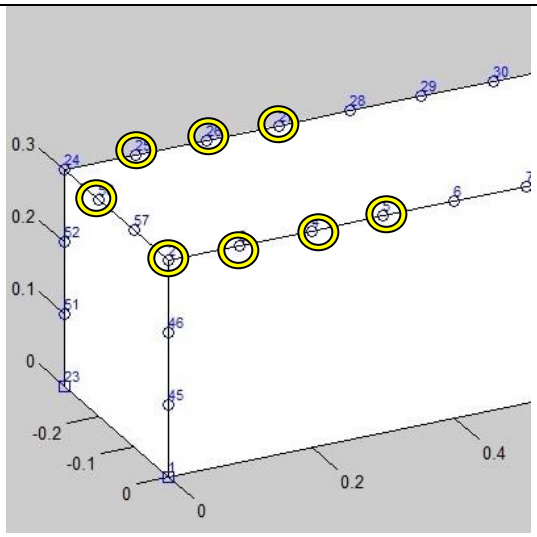

Set 2

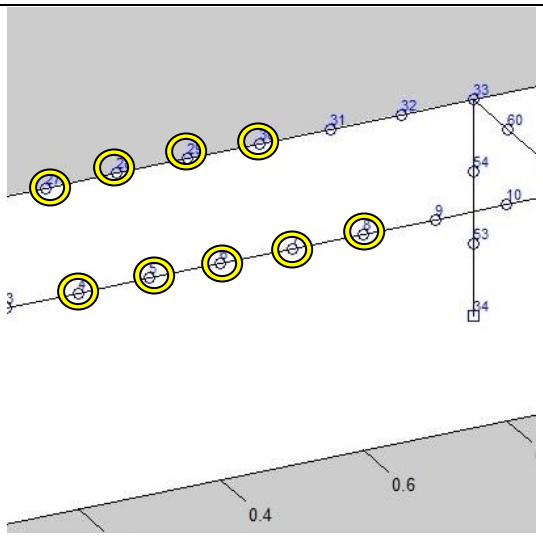

Set 3

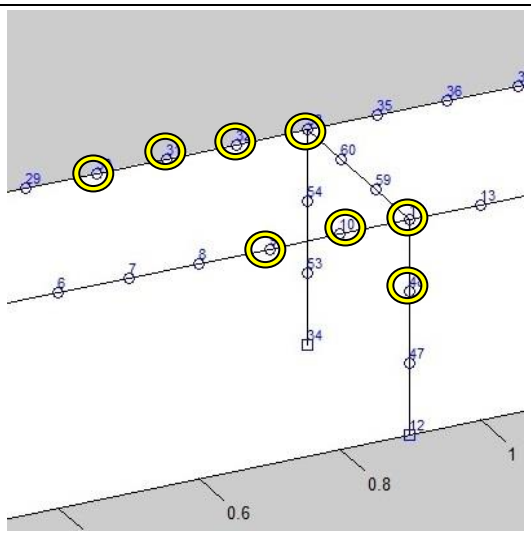

Set 4

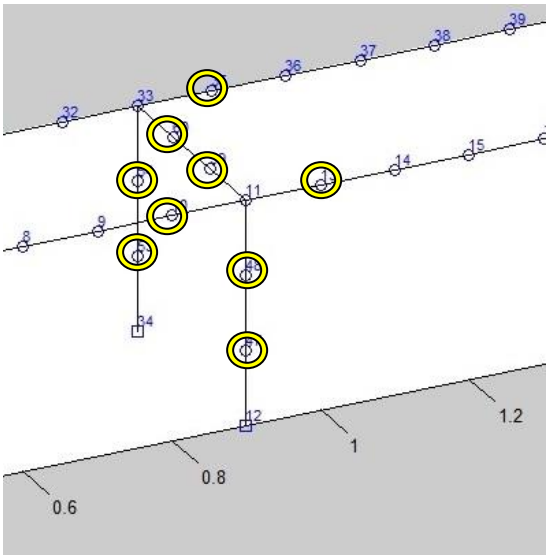

Set 5

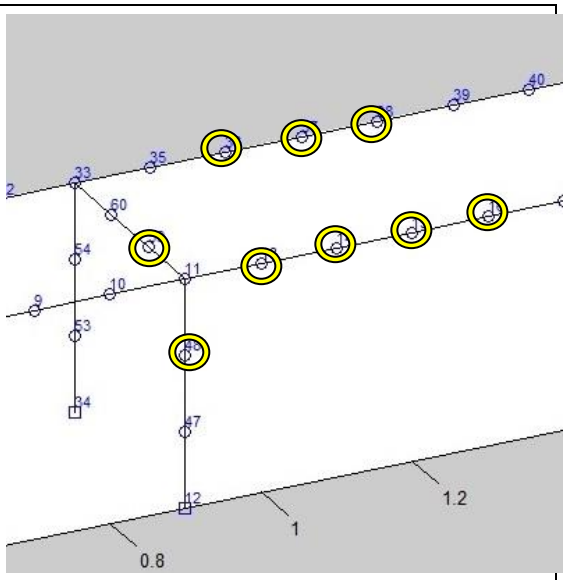

Set 6

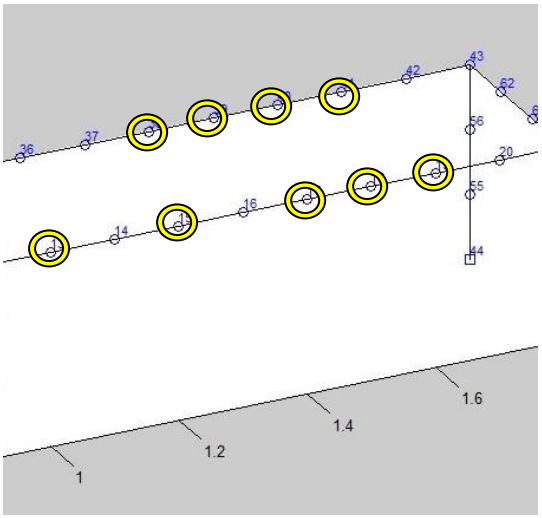

Set 7

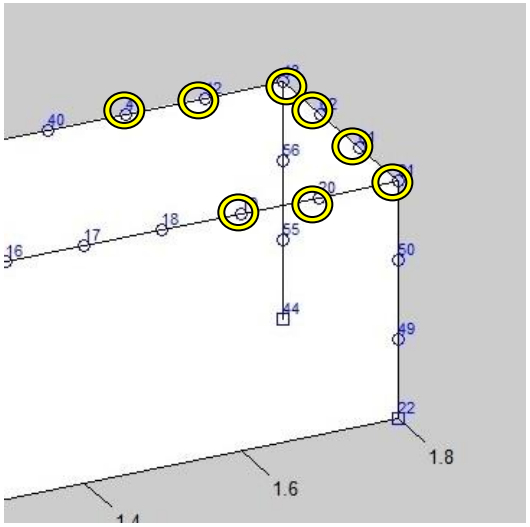

Set 8

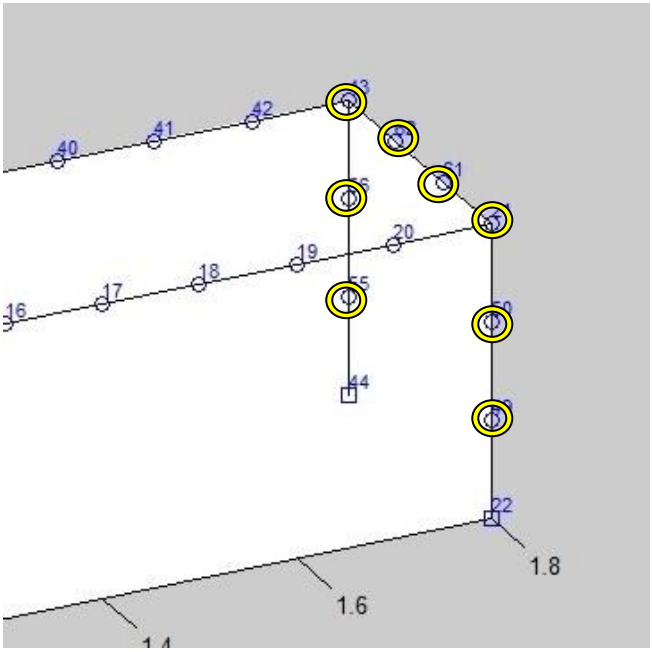

Set 9

Figure 4.9: Placements of accelerometers

4.2.3 Data Acquisition System

Data acquisition system is used to collect signals generated by sensors, and transmit the converted signal to the computer for analyzing. NI CompactDAQ 8-Slot USB Chassis with four NI 9234 analog input modules were used as data acquisition system in this project (Figure 4.10).

The computer with LabView software was used to control the measurement immediately, as it can convert the measured vibration into time and frequency domain data. Therefore, immediate checking can be carried out to see whether the data is reasonable or not, which can identify the capability of the used accelerometers and cables (Figure 4.11)

Figure 4.10: Analog Input Modules

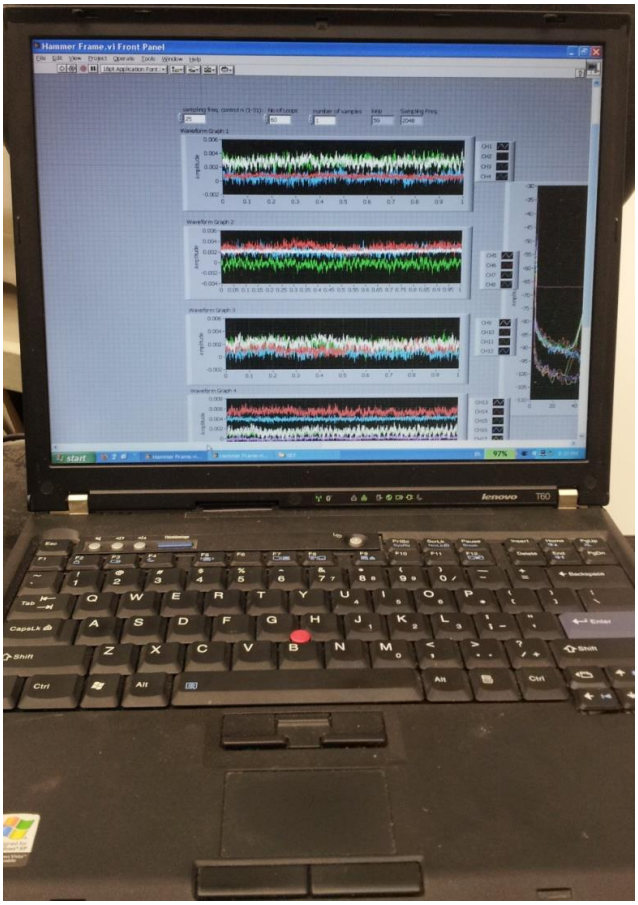

Figure 4.11: Computer with LabView

However, the used would be different in a real long-span bridge due to the limitation of length of cables. Therefore, the sensors should be divided into groups. The data from local sensors would be collected by local acquisition units and then transmit to the central database servers for processing.

4.3Description of loading and damage

The loading would be simulated by using an impact hammer. Since the applied loading was not recorded during the experiment, the vibration can be considered as ambient type. For each measurement set, random loadings were applied on x, y and z direction in a few selected nodes.

Because of the characteristics of simulated damage (Figure 4.12), the data collected under x-direction force was used for correlation. It is due to the changes in the second moment of area. The cross section of beams is defined as Figure 4.13, and the equation of moment of area can be expressed as:

$$I_x = \iint_A y^2 dxdy = \frac{bh^3}{12} \quad (4.1)$$

$$I_y = \iint_A x^2 dxdy = \frac{hb^3}{12} \quad (4.2)$$

Equation 4.1 and 4.2 are the second moment of area for rectangular section only. From the equations, the cross sectional depth value affects the second moment of area the most, which is h for x axis and b for y axis. According to the size of the damage (Figure 4.12), the reduction of cross sectional width b is larger than that of cross sectional depth, which means the second moment of area about y-axis is reduced a lot due to the damage. As a result, the variations of vibration in x-direction should be larger, so data collected under x-direction force is better for

damage localization.

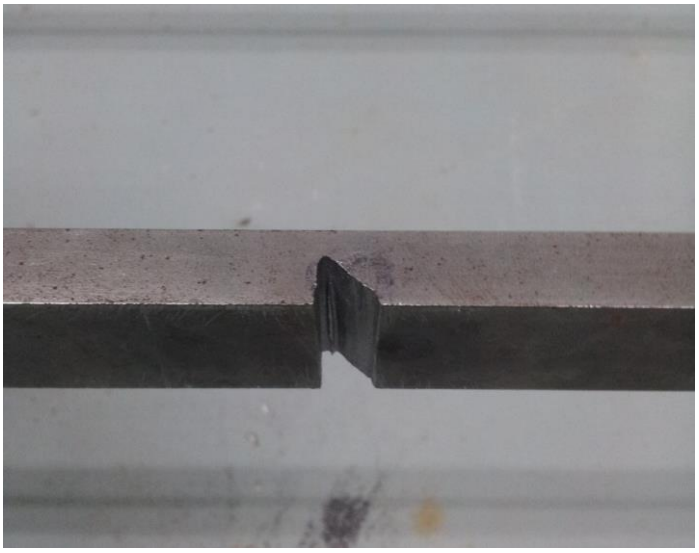

Figure 4.12 Induced damage at node 6

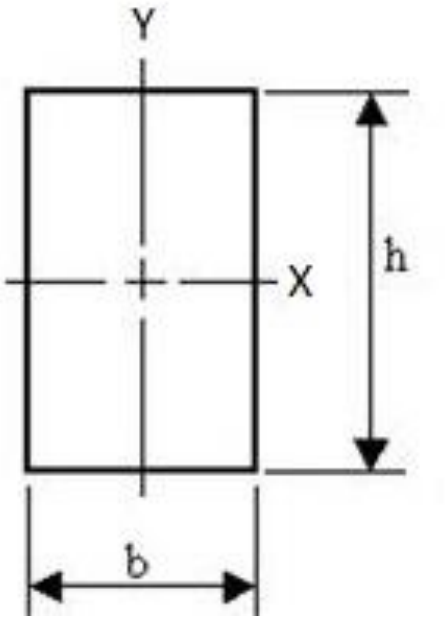

Figure 4.13: Cross-section of beams

4.4Experiment Procedure

The finite element model updating is based on the correlation of responses in different conditions such as damaged and undamaged. Therefore, measurement of responses and corresponding finite model updating should be carried out under

undamaged condition to develop a reference model initially. Totally, nine sets of measurement were performed for the complete measurement, and one set of them is showed in figure 4.14. In each measurement, random forces generated by impact hammer were applied on the mid-span of three structural elements: one column, one transverse beam and one longitudinal beam (Figure 4.15).

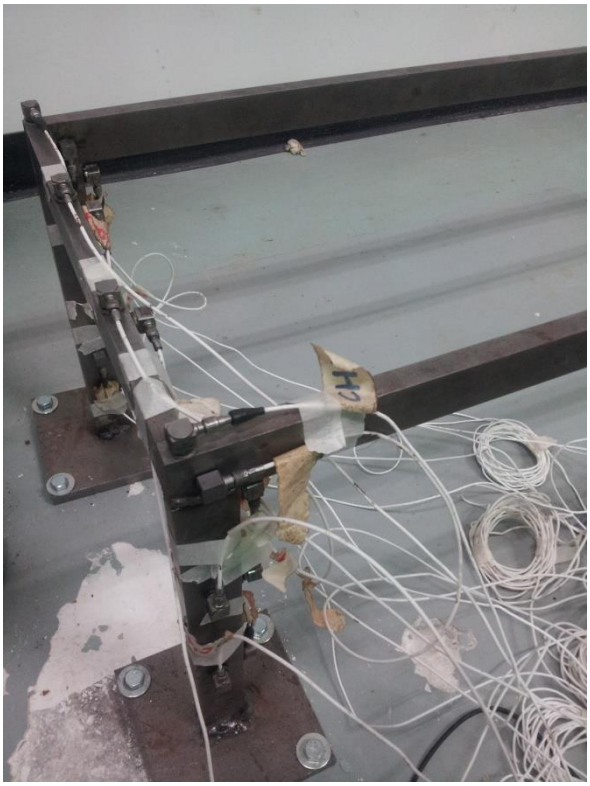

Figure 4.14 Measurement of set 1

		
Force on longitudinal beam	Force on column	Force on transverse beam

Figure 4.15: Force on beams and column

The response were recorded by accelerometers and transmitted to the computer for processing. The accelerometers were installed on each node mentioned in Chapter 4.2.2, connected to the NI 9234 analog input modules through charge cables (Figure 4.16). It should be noticed that the installation of accelerometers should be very careful to prevent damages on accelerometers, for example, the cables were fixed on the model to avoid falling of accelerometers (Figure 4.17). Moreover, the orientation of accelerometers should follow the arrow sign to ensure the accuracy of measurement, which is specified in Chapter 4.2.1. The data transmission cable was connected between NI CompactDAQ 8-Slot USB Chassis and USB port of the computer for data processing.

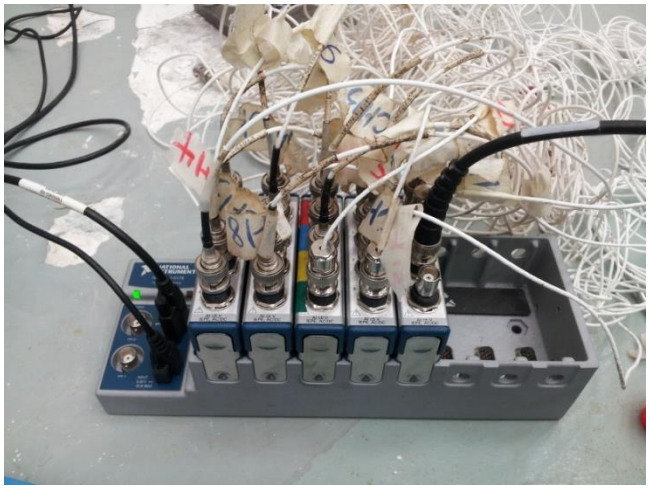

Figure 4.16: Connection between accelerometers and recorders

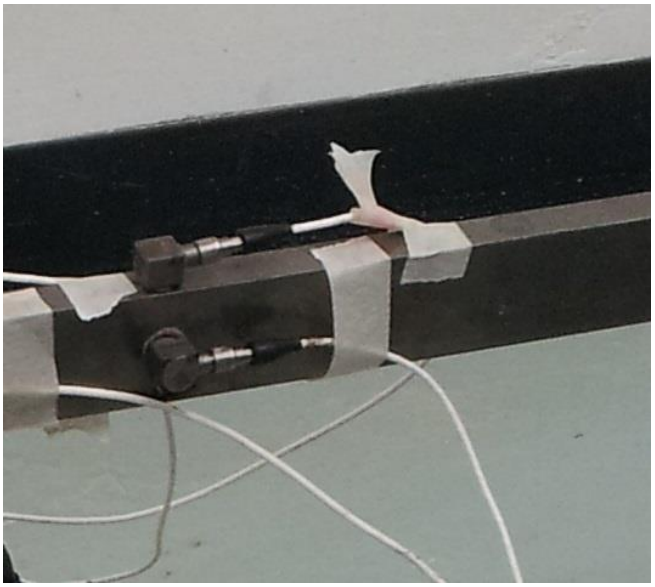

Figure 4.17: Stabilization of accelerometers

The configuration of LabView software should be finished before measurement. In this experiment, eighteen channels were set in the software, and the sensitivity of corresponding accelerometers for each channel was imported for calibration. Besides, the sampling frequency and number of loops were also entered in the program, which are 2048 Hz and 60s respectively. It means that the data was collected 2048 times every second and each set of measurement were last for 60s.

One set of data is used for the finite element model updating, and other sets would be kept for future analyzing if required. The gap between two sets of measurement is around three minutes to prevent the influence from previous loading. And then modal identification was proceeded to obtain useful information such as natural frequencies and mode shapes which were used in the optimization process.

A crack (Figure 4.12) was induced on the longitudinal beam after the measurement and optimization process for undamaged condition. The same procedures described in previous paragraphs were repeated for the measurement of responses of the damaged model.

4.5 Chapter Conclusions

This chapter demonstrates all the used equipments and procedures in vibration measurement, so that to illustrate the correct direction in measurement and avoid making of mistakes during experiment. And the current condition of model also described briefly to ensure the accuracy in simulating finite element model.

CHAPTER5: MODAL IDENTIFICATION

5.1 Output-only Modal Identification Method

There are two common types of vibration tests, ambient test and forced vibration test. The ambient vibrations are always induced by loading without known values such as winds, water flows, traffic loads and earthquakes. In contrast, the loading values are known in forced vibration test.

In a real situation, compared with the forced vibration test, ambient test has some valuable advantages. First, its cost is relatively cheaper than that of forced vibration test because the ambient test does not require any large and heavy excitation equipment such as large shakers or drop weights. Second, the process of ambient vibration test would not affect the operating condition of the bridge as it does not apply any extra loading on the structure. In this thesis, forces with unknown magnitudes were used to simulate ambient test in the real situation.

The modal identification approach which presented by S.K. Au (2011) would be used in this thesis. In this method, modal identification is performed by using Fast Fourier Transform (FFT). The range of measured time domain data around the modes would be selected for modal identification in FFT. And then, comparison of mode shapes would be carried out based on the MAC values between assembled mode shapes. The modal identification and model updating process were carried out by using MATLAB in this thesis as it is a powerful tool that can perform rapid calculations; time can then be saved.

5.2 Extracting Data & Mode Identification

Initially, only the measured time domain data was measured by accelerometers, and the frequency domain data was missing. However, it is necessary to obtain the possible frequencies of each measured mode for the processing of modal identification program. Therefore, FFT was used to transform the non-periodic time domain data into a frequency domain, and this function is originally installed in MATLAB. According to Appendix A.1, the MATLAB code was written to carry out the mentioned processes.

In the beginning, the time domain data was extracted and selected for mode identification. According to Figure 5.1, the changes in acceleration are significant within only part of the samples. Therefore, re-sampling was then carried to extract data with obvious acceleration changes. In this case, samples were selected from the sample with largest acceleration changes until sample number around 50000 was reached. Over half of samples were reduced, which leads speeding up of mode identification processes. Afterwards, FFT was proceeded to get initial guess frequencies for identification. All time domain data from eighteen channels were transformed into frequency domain data, and the transformed data was then averaged for graph plotting (Figure 5.2). Ten modes were selected randomly, and they are also the considered modes in the optimization process.

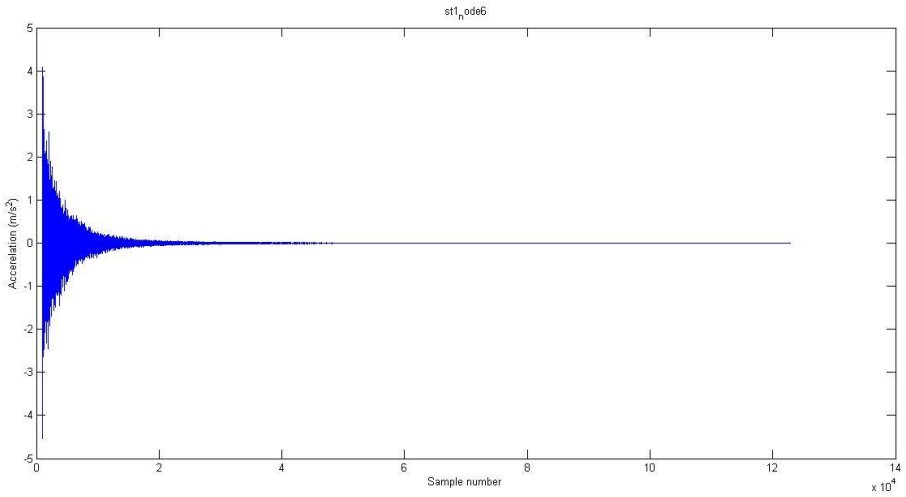

Figure 5.1: Time domain data

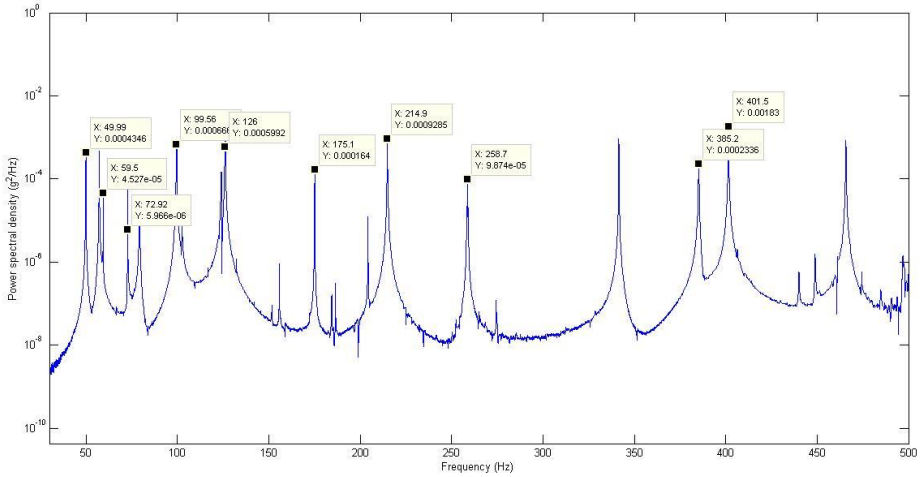

Figure 5.2: Frequency Spectrum/Frequency domain data

For the identification process, all the saved data such as changes in acceleration, initial frequencies and steps size between samples were imported in other MATLAB code for mode identification. In Appendix A.2, the code would automatically generate required input parameters for the processing of the mode identification function, and ten considered modes would be identified. Due to the size of this function, it was not showed in this thesis.

The above extracting and identifying procedures were repeated eight times more

to obtain full sets of data. It should be noticed that the considered modes should be the same in each set of mode identification to ensure the accuracy of the optimization.

The frequencies of considered modes for each set of data are showed below:

Undamaged Data (in Hz):

	Set 1	Set 2	Set 3	Set 4	Set 5	Set 6	Set 7	Set 8	Set 9
Mode 1	49.99	49.84	49.61	49.76	49.85	49.74	49.76	49.95	49.96
Mode 2	59.48	59.29	58.90	59.34	59.45	59.14	59.08	59.44	59.48
Mode 3	72.85	72.57	72.26	72.73	72.83	72.49	72.26	72.75	72.84
Mode 4	99.59	99.74	99.79	99.90	100.01	99.80	99.82	99.44	99.53
Mode 5	126.16	126.26	126.16	126.17	126.11	126.11	126.09	126.01	125.93
Mode 6	174.99	174.22	174.13	174.30	174.84	174.32	174.09	174.67	175.13
Mode 7	214.92	214.30	214.02	214.31	214.94	214.27	214.08	214.62	214.83
Mode 8	258.70	257.96	257.71	258.00	258.30	257.71	257.30	258.09	258.46
Mode 9	385.24	384.64	384.82	385.27	385.87	384.70	384.82	384.08	385.17
Mode 10	401.52	399.88	399.80	399.92	400.35	399.63	399.41	400.28	401.30

Table 5.1: Frequencies for each considered mode of undamaged model

Damaged Data (in Hz):

	Set 1	Set 2	Set 3	Set 4	Set 5	Set 6	Set 7	Set 8	Set 9
Mode 1	49.75	49.58	49.31	49.53	49.64	49.52	49.56	49.75	49.75
Mode 2	58.87	58.66	58.27	58.75	58.90	58.65	58.53	58.84	58.92
Mode 3	72.03	71.76	71.49	71.94	72.02	71.67	71.37	71.88	72.02
Mode 4	99.11	99.35	99.38	99.60	99.87	99.47	99.53	99.17	99.22
Mode 5	125.26	125.24	125.12	125.10	125.03	125.00	125.02	124.94	124.92
Mode 6	174.63	173.69	173.55	173.80	174.31	173.78	173.64	174.06	174.81
Mode 7	213.95	213.32	212.61	213.29	213.96	213.27	213.14	213.56	213.84
Mode 8	258.55	257.76	257.47	257.82	258.33	257.35	257.23	257.80	258.37
Mode 9	379.78	379.15	378.84	379.65	380.15	378.67	378.74	378.04	379.03
Mode 10	398.70	397.02	397.18	397.43	398.36	397.44	396.96	397.94	398.71

Table 5.2: Frequencies for each considered mode for damaged model

From the tables 5.1 and 5.2, it shows that most considered modes between two stages are similar except for the ninth one. It was because that this frequency is not available in the frequency spectrum of damaged model, so another initial guess frequency was used for identification. The reason of absent of frequency may be due to the damage that destroyed the vibration properties of the model.

5.3 Combine of Mode Shapes

The major step for this modal identification approach is to combine each set of data to represent mode shapes of the whole structure. During the measurements, there are no fixed DOF throughout entire tests, but at least one reference DOF was measured between each sets of data. Therefore, the mode shapes can be correlated set by set. According to the research of Au (2011), the equations of optimal mode shape values for reference DOF and non-reference DOF are demonstrated in his thesis, and the objective function is set by make use of MAC. And some mathematical modifications are introduced to reduce the size of the problem. Based on the achievements of this research, a MATLAB code was written to combine the different sets of mode shape, which is showed at Appendix A.3.

From the beginning of this code, nine “Location” matrices were developed to represent the relationship between the data channels and corresponding DOF specified in the reduced numerical model. The row numbers are the corresponding channel, and the column numbers are the DOF in reduced numerical model. The value “1” points out which DOF is corresponding to the channel. In fact, the total number of DOF in the numerical model should be 336 instead of 118 in the “Location” matrices. It was because that some DOF cannot be measured such as

rotational DOF, and the combining process does not allow for DOF without measured data, so the total number of DOF should then be reduced. Apart from the assigning function, “Location” matrices can also state the reference DOF as there are many overlapped values between matrices that would be make use of in the combining process.

After the assigning of channels, the mode shapes were combined based on the computer codes developed from the simplified concepts introduced by S.K. Au (2011). In his theory, the proposed objective function is nonlinear and multi-dimensional, so iterative approach such as Least-Squares was used instead of direct calculation. In addition, the mode shapes were also normalized while combining.

5.4 Mode Shape Normalization

Normalization of mode shape is necessary for the correlation of mode shape between damaged and undamaged states can be carried out. The Euclidean norm of each set of mode shape would be calculated, and then the mode shape would be divided by the calculated Euclidean norm. As a result, mode shapes can be normalized. The normalization code was written and showed in Appendix C.1.

5.5 Modal Assurance Criterion

Mac is used to calculate the similarity between two mode shapes. The higher the MAC value, the higher the convergence of mode shapes. The MAC code was developed based on the equation 2.1, and it was attached in appendix C.2

$$\mathrm{MAC}[\Phi_{ti}\,,\ \Phi_{ei}] = \frac{\left|(\Phi_{ti})^{T}(\Phi_{ei})\right|^{2}}{[(\Phi_{ti})^{T}(\Phi_{ti})][(\Phi_{ei})^{T}(\Phi_{ei})]} \qquad (2.1)$$

5.6 Chapter Conclusions

Modal identification is explained in this chapter. The approach to identify useful modal parameters from raw data is demonstrated, and some techniques used in analyzing of data are studied such as mode shape normalization and modal assurance criterion. Therefore, accurate modal parameters can be obtained for model updating and damage detection.

CHAPTER 6: DAMAGE DETECTION OF THREE-DIMENSIONAL SCALED BEAM-BRIDGE FRAME

6.1 Simulated Finite Element Model

For the correlation between experimental and theoretical responses, a three-dimensional numerical finite element model was developed based on the known geometric information and the assumed structural properties of the model. MATLAB was used for the building up of finite element model, and the code was showed in Appendix B.1. All the dimensions used in this finite element model are according to the values presented in Chapter 4. For unknown structural properties such as density, young's modulus and shear modulus of steel, they are assumed to be 7800 kg/m^3, 210 GPa and 80 GPa respectively.

The code in Appendix B.1 is used to form the finite element model. Necessary information such as coordinates of nodes, points for locating local bending plane for each element, connectivity of the elements and the structural properties were imported for further stiffness calculation. Afterwards, function "frame3d_modify" developed on the basis of matrix stiffness method was used to calculate three-dimensional frame system stiffness matrix by importing necessary information that mentioned above. For the scaled beam-bridge frame model, there are several conditions were considered before the formulation of information matrices.

1. The translational and rotational DOF at supports are restrained.
2. The connection flexibility of each element is considered as rigid joint.

By considering the above conditions and following the requirement specified in Appendix B.1, four essential information matrices “node”, “point”, “elem” and “prop” were formed and showed in Appendix B.1.

After that, the calculated system stiffness and mass matrices were used to find out the corresponding eigenvalues and eigenvectors. In physical, they are the circular natural frequencies and mode shapes of a structure respectively. To be concluded, the code in Appendix B.1 utilize the function “frame3d_modify” to form system stiffness and mass matrices, and then default function “eig” or other self-developed function would be used to find out natural frequencies and mode shapes.

6.2 Damage Detecting by Model Updating

6.2.1 Objective Function

In this thesis, frequency residuals and mode shape residuals were selected to form the objective function which is already showed in Chapter 3. The objective function is:

$$\min J = \sum_{i=1}^{N} \left(\omega_f \left| \frac{f_{ti} - f_{ei}}{f_{ei}} \right| \right) + \sum_{i=1}^{N} (\omega_m |1 - MAC|) \qquad (3.6)$$

After the applying of weighting factors in Chapter 6.2.3, the decided objective function is:

$$\min J = \sum_{i=1}^{N} \left(\frac{1}{2} \left| \frac{f_{ti} - f_{ei}}{f_{ei}} \right| \right) + \sum_{i=1}^{N} \left(\frac{1}{2} |1 - MAC| \right) \qquad (6.1)$$

The MATLAB code for the objective function was written and attached in appendix D.1. Firstly, the trials of updating parameters would be assigned into the simulated model (Appendix B.1) to get corresponding theoretical natural frequencies and mode shapes. And then, the theoretical mode shapes would be reduced in size and normalized for the correlation between damaged and undamaged models. MAC is used to match mode shapes and indicates which theoretical modes are highly matching with the experimental mode shapes. At the end of the code, the percentage error "Jv" value would be calculated to show the level of optimization, and it should be as smaller as possible.

6.2.2 Updating Parameters

Selection of updating parameters should be considered very carefully as it may heavily affect the accuracy of the optimization. According to the matrix stiffness method, natural frequencies and mode shapes of the structure are heavily influenced by the system stiffness and mass matrices, so these two matrices should be first considered. In this project, the volume of induced crack is relatively small compared with the whole structure, so the changes in mass matrix may be very small, and it can be considered as constant before and after the induce of damage. For the system stiffness matrix, refer to Chapter 4.2, the second moment of area would be largely decreased due to a reduction in cross section area of longitudinal beam, so it can be selected as updating parameter. Since young's modulus has the same effect on the bending stiffness (Eq. 6.2), it can also be the updating parameter.

$$K = \frac{EI}{L^3} \tag{6.2}$$

The number of updating parameters should also be considered. It was because ill-condition problem may be occurred if the considered modes are less than the updating parameters. According to the formulated property matrix showed in appendix B.1, if the second moment of area is selected as updating parameter, changes in I_x and I_y should be considered simultaneously as the crack is not affecting the second moment of area only in one direction. Therefore, young's modulus was selected to reduce the number of updating parameter.

6.2.3 Weighting Factors

According to Chapter 3.2.3, the frequency residuals can normally multiply with a higher weighting factor that that of mode residuals. However, since there is no standard for the selection of weighting factor of each modal parameter, weighting factor would be set as 0.5 for both residuals in this thesis.

6.2.4 Optimization Algorithm

The optimization algorithm selected to minimize the objective function (Eq 6.1) is the active-set algorithm which can be used for general nonlinear optimization. Besides, trust-region reflective algorithm is also a common method, but it requires a user define gradient equation that is not formulated in this thesis. Therefore, active-set algorithm was selected for optimization.

The optimization process was performed by using function "fmincon" in the MATLAB optimization Toolbox (Mathworks, 2013). The input parameters are the objective function, initial trials of updating parameters, lower bounds and

upper bounds. The code for using “fmincon” is showed in Appendix D.2, it initially generates random trials of updating parameters, and it would be assigned into the code for the objective function to proceed minimizing approach that mentioned in Chapter 6.2.1. This function would iterate the updating parameters within the boundaries between 0.001 and 2.5 to achieve minimum Jv value in the objective function. It is noticed that the number of trials should be as much as possible to obtain the global minimum.

6.3 Model Updating and Damage Detection

The first step of model updating is to assign the updating elements into groups. In this model, there are three types of structural elements such as columns, transverse beams and longitudinal beams. One updating parameter was assigned to each pair of column; one was assigned to three transverse beams and one was assigned to each longitudinal beam. The assignment of updating parameters is showed in Figure 6.1.

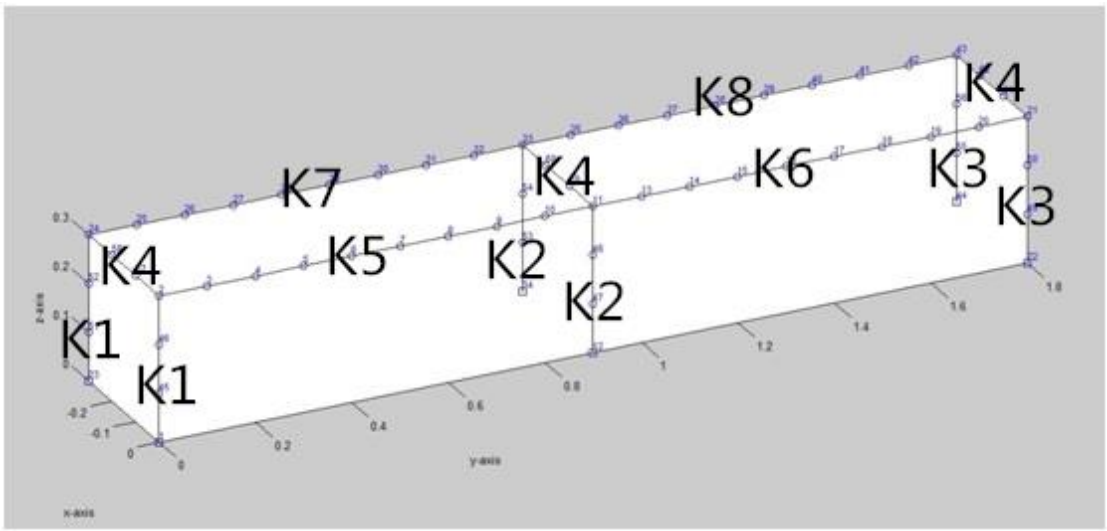

Figure 6.1: Assignment of updating parameters

After the modal identification presented in Chapter 5, measured frequencies and mode shapes can be used in the correlation process. And then the codes for the objective function, optimization and simulate model (Appendix D.1, D.2 and B.1) would be used for model updating. By comparing the differences in updating parameters between undamaged and damaged model, the damage can then be localized.

6.3.1 Model Updating of Undamaged Model

During the optimization process, over 1000 sets of trials of updating parameters were used to achieve global minimum. The result shows that over 200 sets of trials had achieved the minimum Jv value 0.1352, and their corresponding updating parameters are very similar to each other. Therefore, average of updating parameters was taken. From table 6.1, updated young's modulus for all elements is decreased, which is reasonable. First, the actual young's modulus for steel elements is always smaller than the preferred one because of the imperfection of manufacturing. Second, the long steel bars produced in the factory require further cutting to formulate suitable structural elements. Furthermore, except for the second pair of columns, the decreasing of young's modulus in columns and transverse beams are much larger than that of longitudinal beams. The connection properties may be one of reasons for this phenomenon. From figure 6.2, it shows that one long beam is actually divided into two longitudinal beams in the finite element model so the connection should be much stronger than other elements as they were just welded. As a result, the transverse beams and columns may be relatively weaker in the finite element model.

Figure 6.2: Joint Property

Jv	K1	K2	K3	K4	K5	K6	K7	K8
0.1352	0.7631	0.9627	0.8243	0.6943	0.9297	0.9749	0.9490	0.9818

Table 6.1: Results of updated parameters

To evaluate the correlation of frequencies and mode shapes, numerical comparison is made to present the accuracy of mode updating which is showed in table 6.2. It shows that most frequencies are well paired as they have only 1% error, except for frequencies at second and sixth considered modes that have around 2-3% error. For the MAC values, most of the mode shapes are good related apart from the fifth mode which is only 93.247% matched with the experimental mode shape. However, the correlation of frequencies and mode shapes are still very successful as there is only one parameter with more than 5% error. More direct evaluation of correlation is showed in figure 6.3 and 6.4 for frequencies and mode shapes respectively. Figure 6.3 clearly shows the discrepancy in two stages by emphasizing the level of errors as the size of gaps from the diagonal line. Most of the frequencies are nearly laid on the diagonal line, so the theoretical frequencies

are updated accurately. For figure 6.4, the x-axis is the experimental modes, and each color showed in legend is representing the theoretical modes. The level of matching is displayed by z-axis in percentage. The graph illustrates the orthogonal conditions between theoretical and experimental mode shapes, and the highest MAC value clarifies which mode is closely matched.

	Experiment (Hz)	Initial FE model (Hz)	Error (%)	MAC (%)
Mode 1	49.82800	49.82801	0.000003	99.679
Mode 2	59.28839	61.44059	3.630051	99.609
Mode 3	72.62213	72.98457	0.499082	99.618
Mode 4	99.73562	99.73561	-0.000014	93.247
Mode 5	126.1123	126.1917	0.062980	98.755
Mode 6	174.5207	178.2237	2.121812	97.576
Mode 7	214.4781	212.3286	-1.002180	98.553
Mode 8	258.0243	255.9532	-0.802673	99.253
Mode 9	384.9567	384.9567	0.000004	97.444
Mode 10	400.2313	397.6068	-0.655733	98.001

Table 6.2: Comparison of experimental and theoretical modal properties of undamaged model

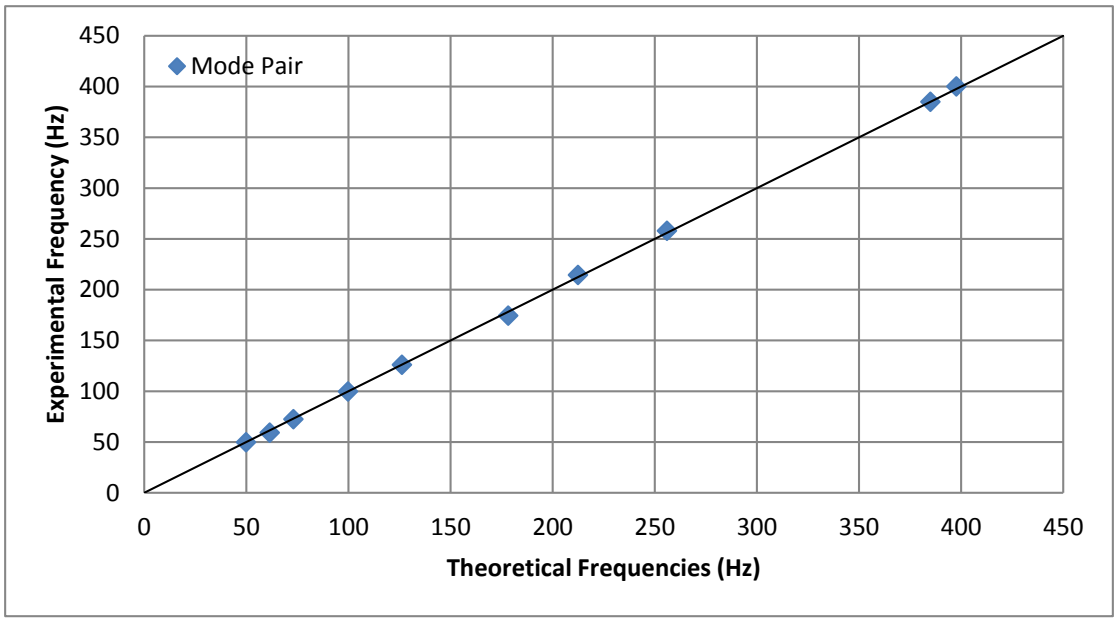

Figure 6.3: Frequency correlation of undamaged model

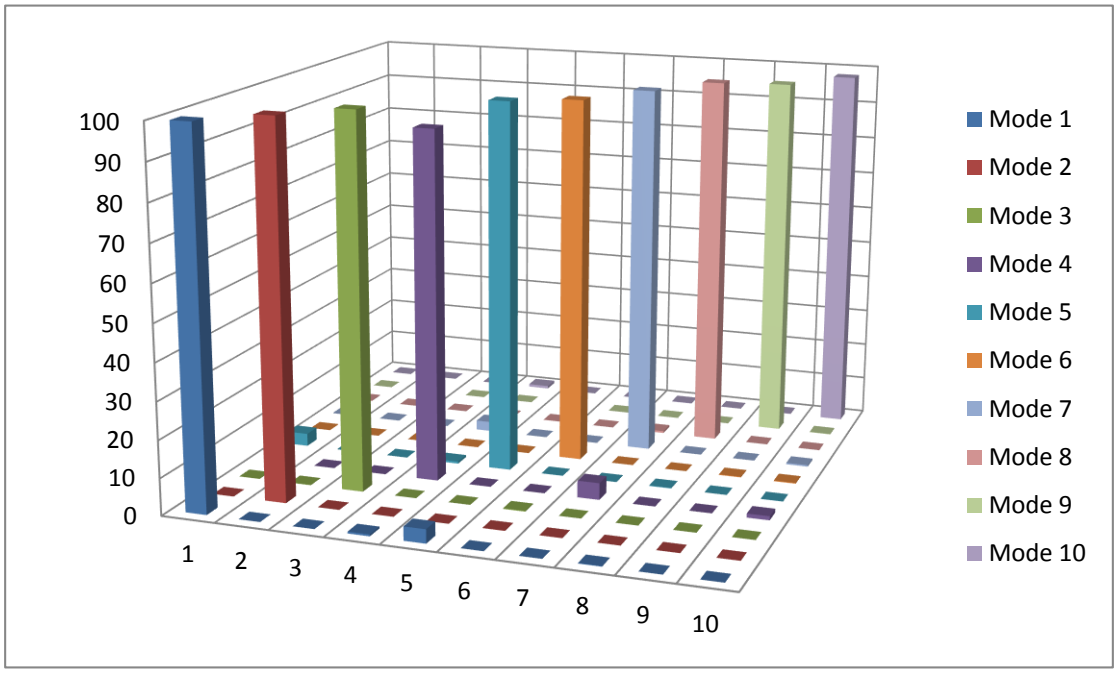

Figure 6.4: Mode shapes correlation of undamaged model

Besides, the experimental mode shapes are expanded to compare with the updated theoretical mode shapes to see whether the vibration shapes are similar or not. Figure 6.5 to figure 6.14 are plotted to show the vibration in each mode, and red line is representing the experimental mode shapes. By

visual inspection, the vibration shapes and curvatures are very similar. To be concluded, the frequencies and mode shapes are updated with little errors so that it can represent the actual model, and can be used in damage detection comparison.

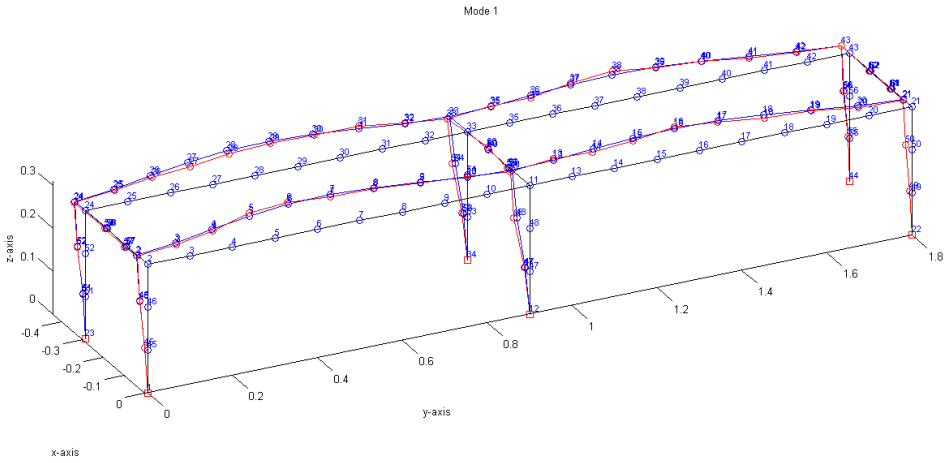

Figure 6.5: Comparison of experimental and theoretical vibration at mode 1 for undamaged model

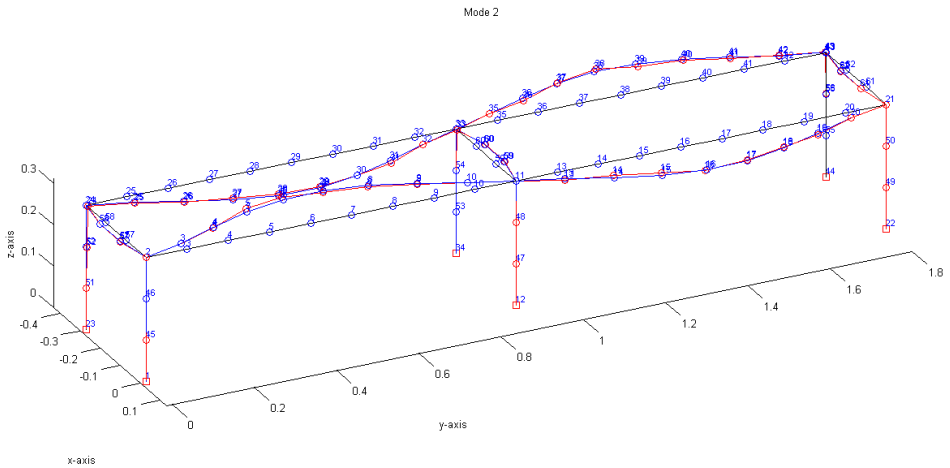

Figure 6.6: Comparison of experimental and theoretical vibration at mode 2 for undamaged model

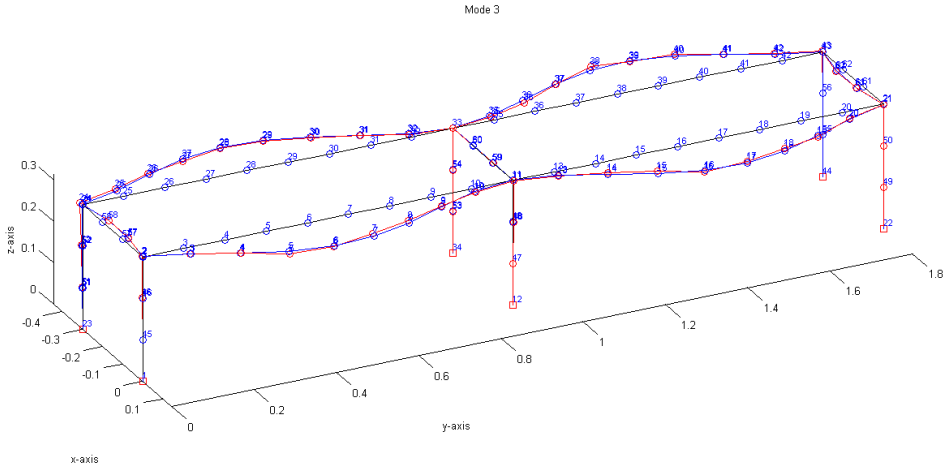

Figure 6.7: Comparison of experimental and theoretical vibration at mode 3 for undamaged model

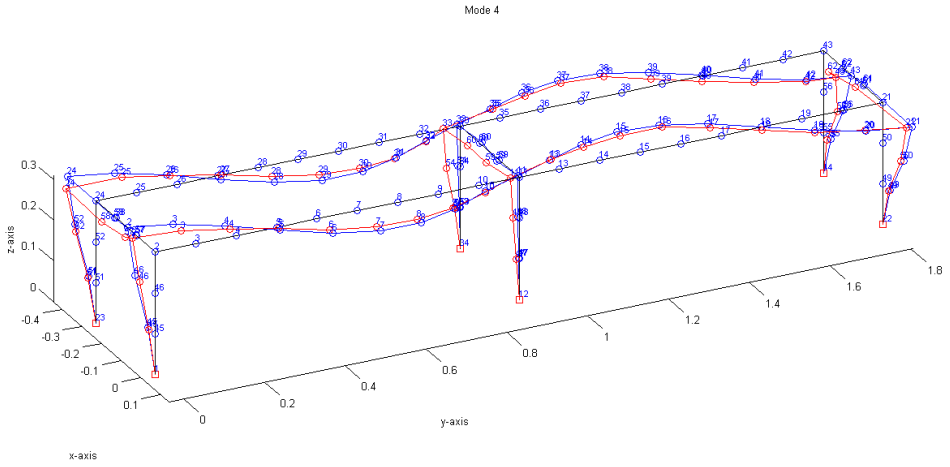

Figure 6.8: Comparison of experimental and theoretical vibration at mode 4 for undamaged model

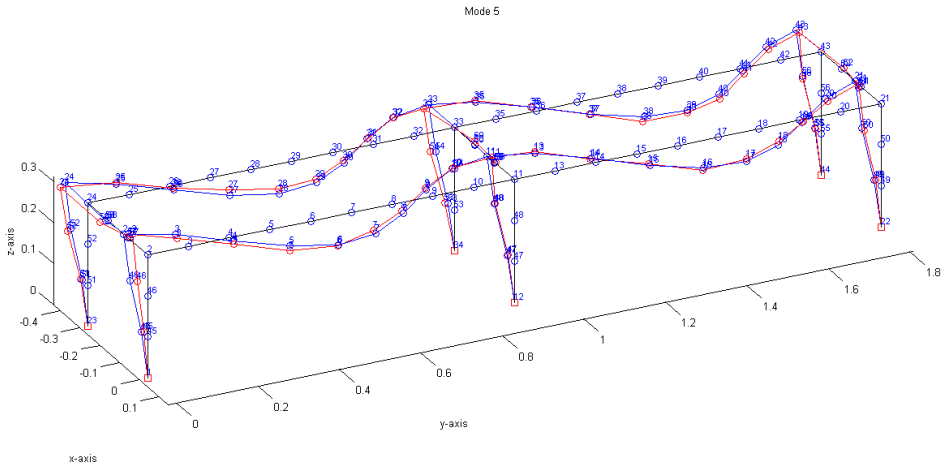

Figure 6.9: Comparison of experimental and theoretical vibration at mode 5 for undamaged model

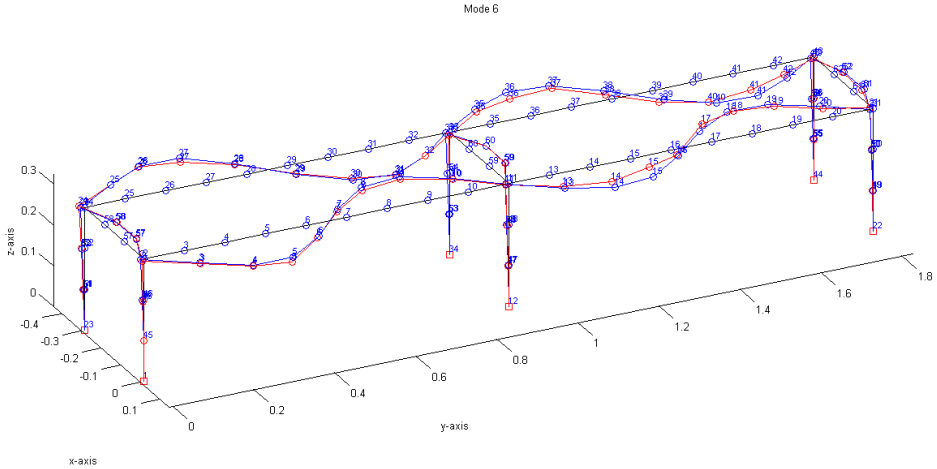

Figure 6.10: Comparison of experimental and theoretical vibration at mode 6 for undamaged model

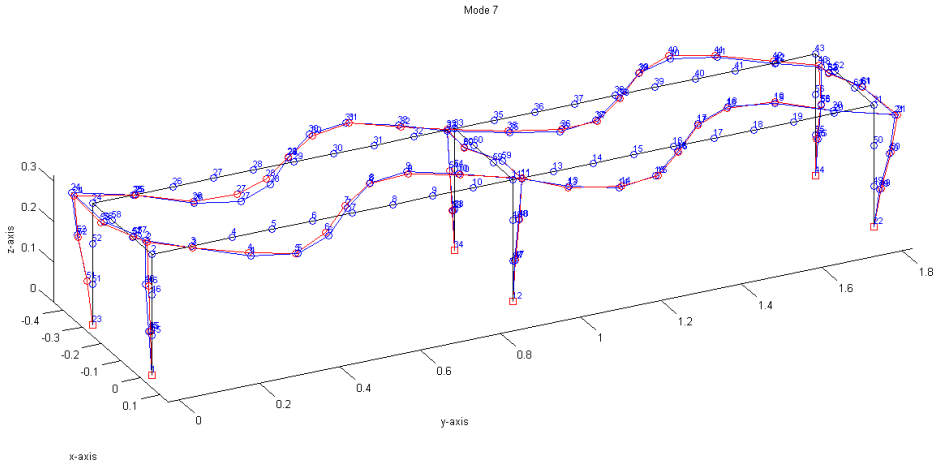

Figure 6.11: Comparison of experimental and theoretical vibration at mode 7 for undamaged model

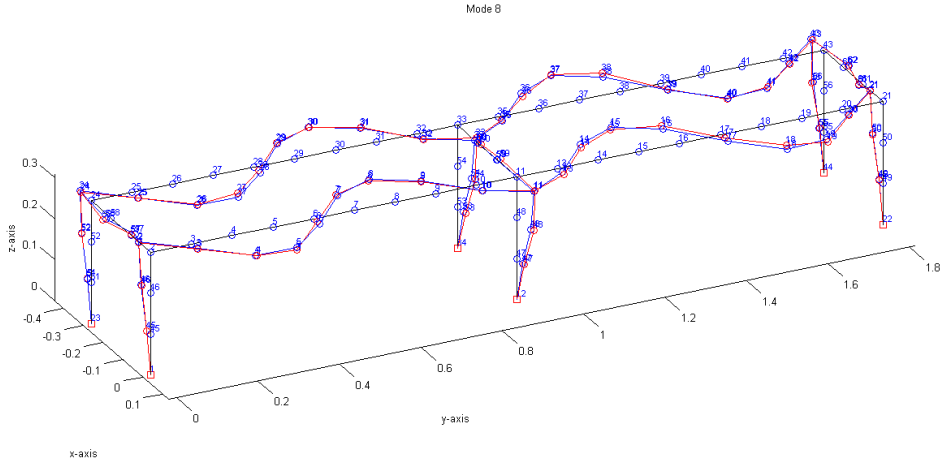

Figure 6.12: Comparison of experimental and theoretical vibration at mode 8 for undamaged model

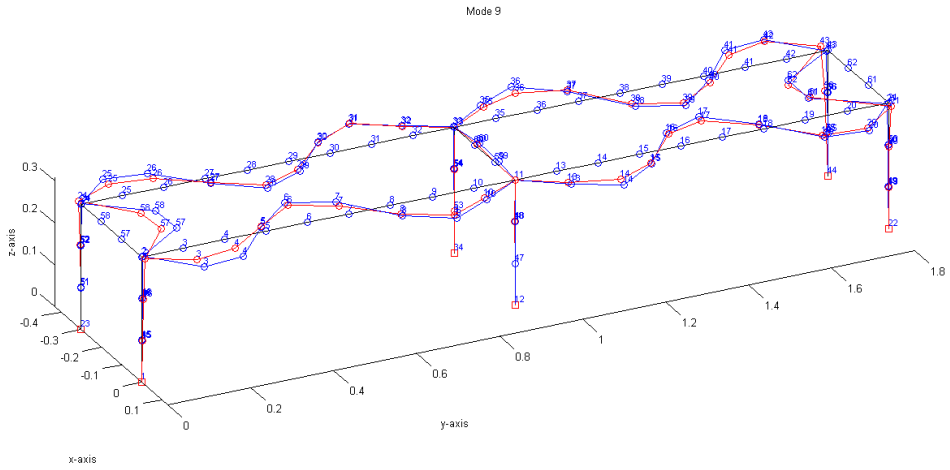

Figure 6.13: Comparison of experimental and theoretical vibration at mode 9 for undamaged model

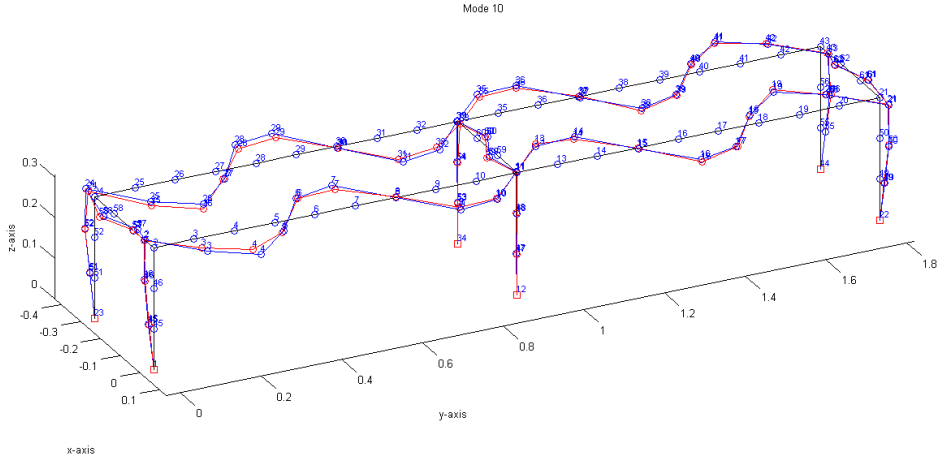

Figure 6.14: Comparison of experimental and theoretical vibration at mode 10 for undamaged model

6.3.2 Damage Detection

After the completion of the model updating for undamaged model, damage was induced in the mid-span of one longitudinal beam stated in figure 6.15. It was assumed that the damage location is unknown, so all structural elements were updated to localize the damage. The initial objective was to localize the

damage as accurate as possible, so updated elements were divided into more pieces that are different to that of undamaged model (Figure 6.15). According to table 6.3, six parameters are decreased by over 10%, and three of them are decreased by around 20% to 40%. However, there are only one damage was induced, so the results are not reasonable. It seems that too many updating parameters are not helpful in damage localization. It was proved by studying from other theses, some researchers mention that the number of updating parameters cannot be larger than the number of considered mode in damage localization.

	Updated parameters for undamaged model	Updated parameters for damaged model	Error (%)
Element 1	0.7631	0.7861	3.0036
Element 2	0.9627	0.9815	1.9593
Element 3	0.8243	0.8959	8.6918
Element 4	0.6943	0.5573	-19.7295
Element 5	0.6943	0.5818	-16.2081
Element 6	0.6943	0.6223	-10.3716
Element 7	0.9297	0.9245	-0.5571
Element 8	0.9297	0.6605	-28.9513
Element 9	0.9297	1.0936	17.6305
Element 10	0.9749	1.2805	31.3446
Element 11	0.9749	0.6083	-37.5994
Element 12	0.9749	1.1703	20.0402
Element 13	0.9490	0.9015	-5.0083
Element 14	0.9490	1.0630	12.0083
Element 15	0.9490	1.0141	6.8539
Element 16	0.9818	1.1177	13.8460
Element 17	0.9818	0.8492	-13.5081
Element 18	0.9818	0.9869	0.5259

Table 6.3: Comparison of updated parameters between undamaged and damaged model

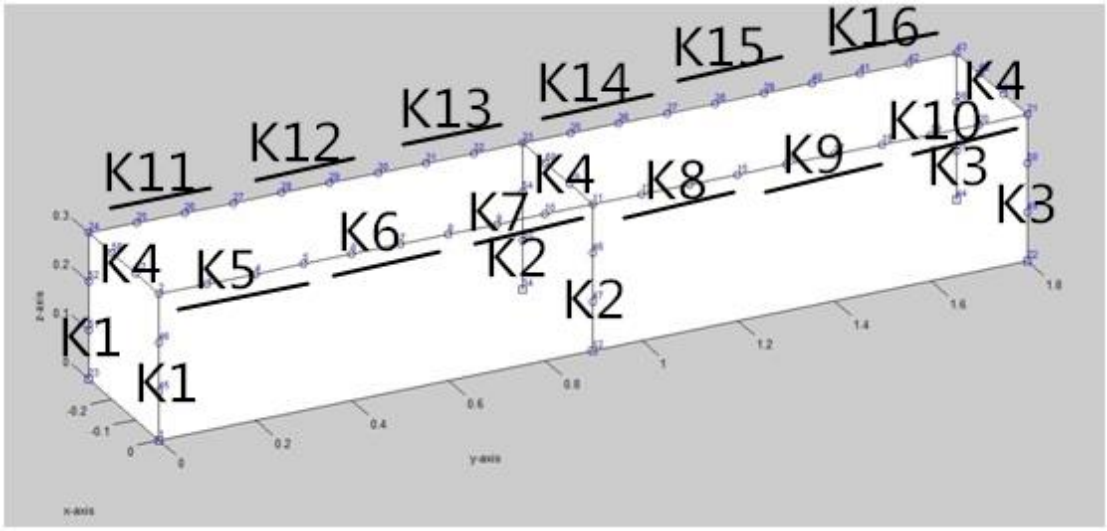

Figure 6.15: Initial assignment of updating parameters for damaged model

Due to the previous problem, an improved approach was used. Firstly, the model was updated with updating parameters same as the undamaged model to find out rough damage location. Secondly, further damage detection was carried out to find out the exact location of the damage.

The correlation results are demonstrated same as the part of undamaged model. For natural frequencies, there are two frequencies (second and eighth modes) with 2-3 % errors and others are closely updated. For mode shapes, the MAC values state that the fifth and sixth modes are updated not enough accurate compared to other modes. Therefore, visual inspection on mode shape vibrations would be carried out later to justify the matching is reasonable or not. From the figure 6.16 and 6.17, all frequencies touch the diagonal line very closely, and all mode shapes are highly matched in the diagonal line, so the correlation is successful numerically.

	Experiment (Hz)	Initial FE model (Hz)	Error (%)	MAC (%)
Mode 1	49.59667	49.59666	-0.0000234	99.42747
Mode 2	58.71023	60.87274	3.6833620	96.12619
Mode 3	71.79733	71.97567	0.2483872	99.48721
Mode 4	99.41135	99.41107	-0.0002784	95.15056
Mode 5	125.0689	125.1435	0.0595956	90.29388
Mode 6	174.0297	175.7448	0.9855334	90.29388
Mode 7	213.4377	210.5036	-1.3747045	98.39369
Mode 8	257.8539	252.7438	-1.9817835	98.53378
Mode 9	379.116	379.116	-0.0000049	97.72096
Mode 10	397.7484	393.6693	-1.0255481	97.94695

Table 6.4: Comparison of experimental and theoretical modal properties for damaged model

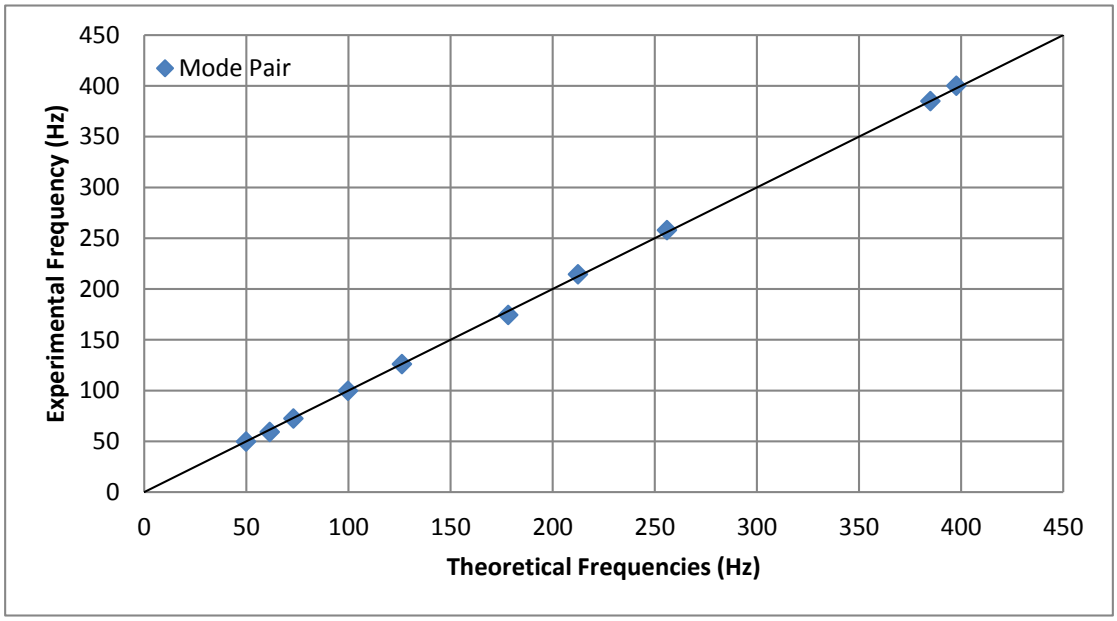

Figure 6.16: Frequency correlation of damaged model

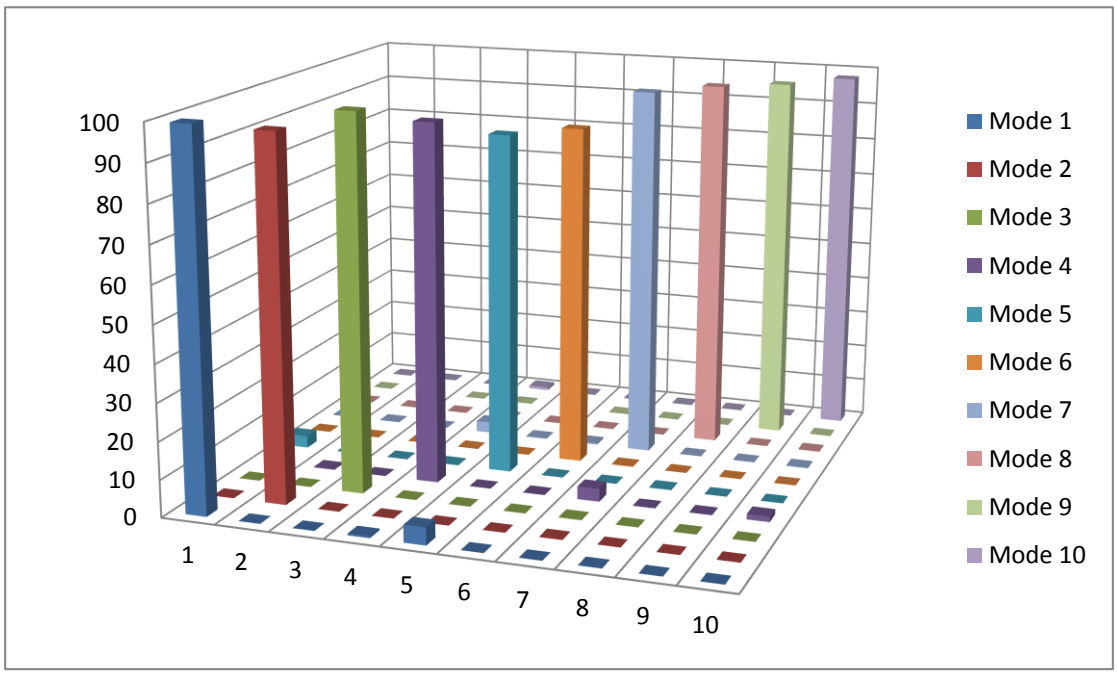

Figure 6.17: Mode shapes correlation of damaged model

From figure 6.18 to figure 6.27, all matched mode shapes have similar vibrations and curvatures, so the problem of MAC values in mode 5 and 6 can be neglected. Therefore, the updated model can be used to represent the current condition of the real model.

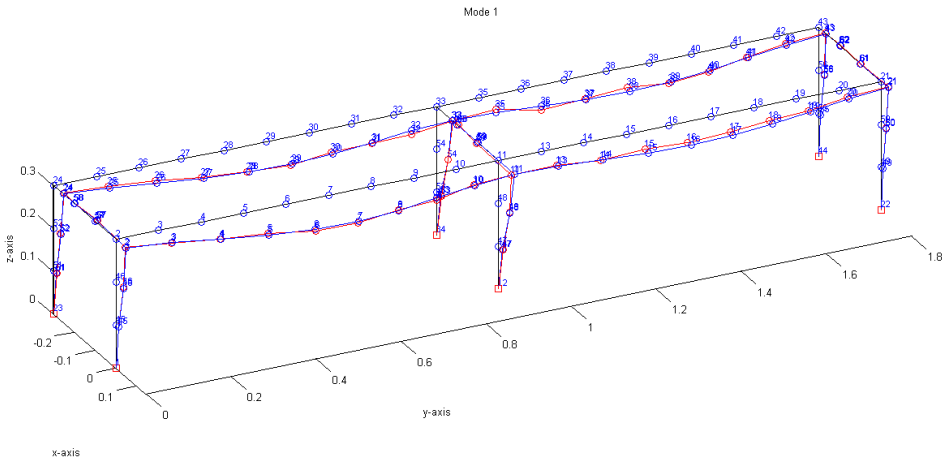

Figure 6.18: Comparison of experimental and theoretical vibration at mode 1 for damaged model

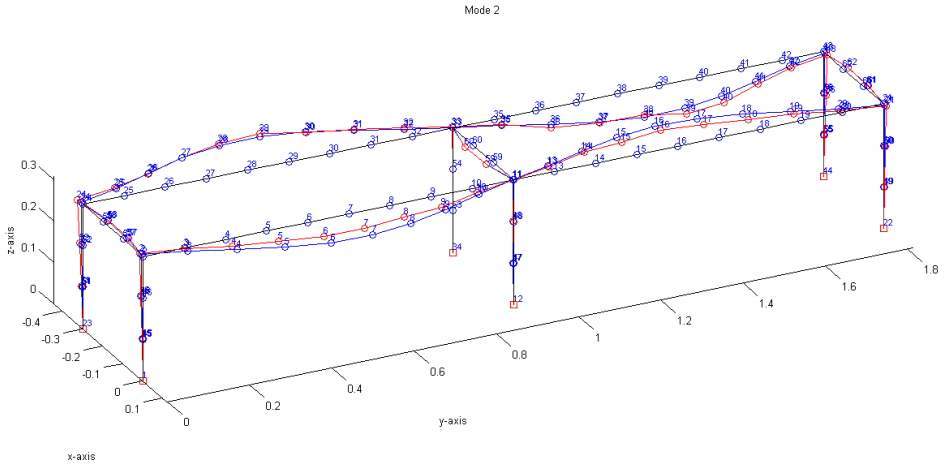

Figure 6.19: Comparison of experimental and theoretical vibration at mode 2 for damaged model

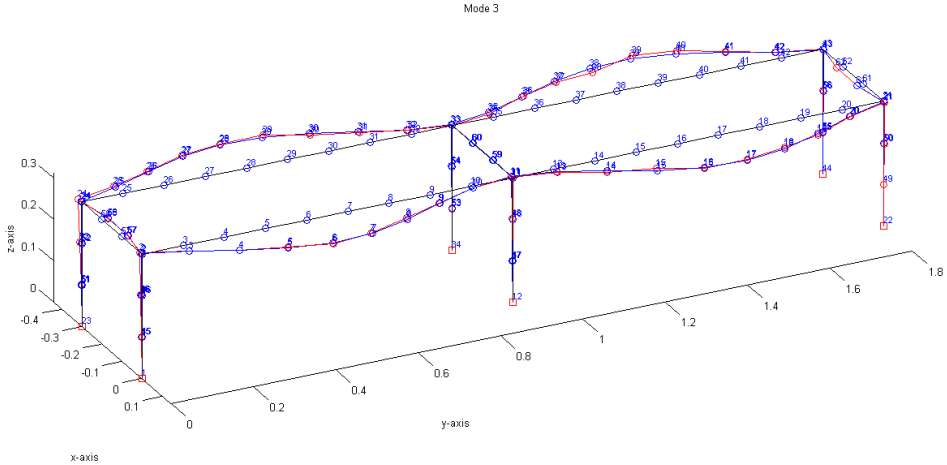

Figure 6.20: Comparison of experimental and theoretical vibration at mode 3 for damaged model

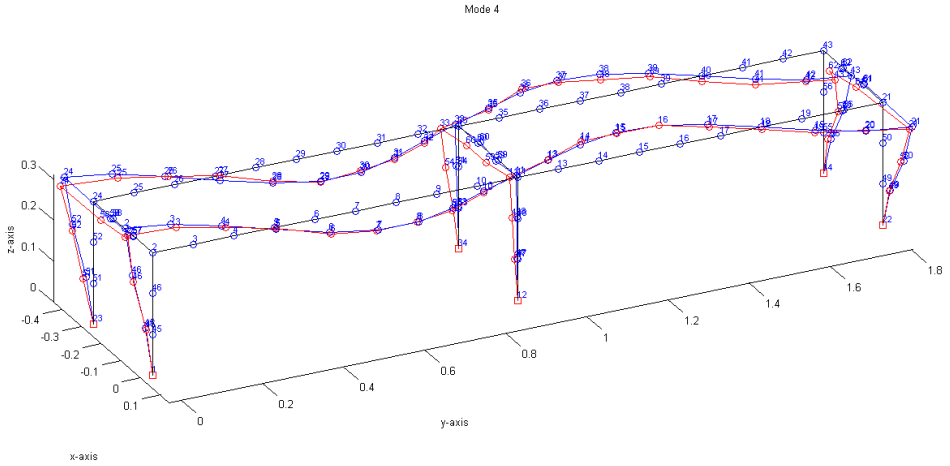

Figure 6.21: Comparison of experimental and theoretical vibration at mode 4 for damaged model

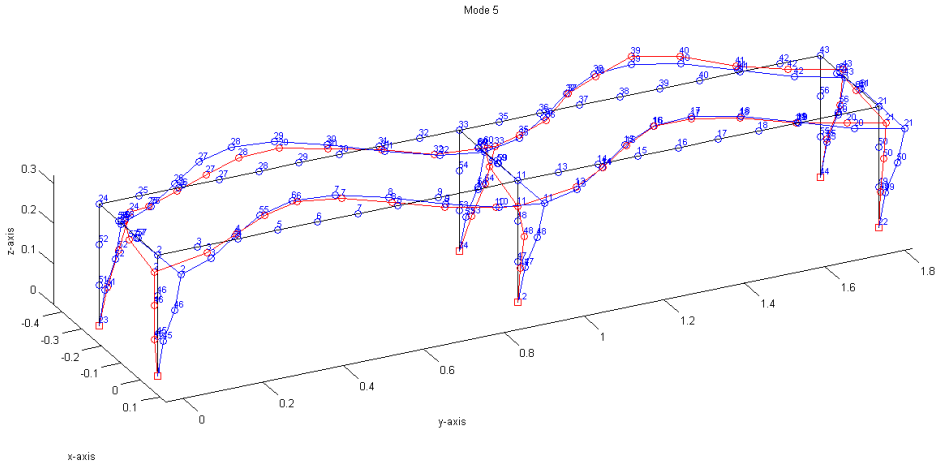

Figure 6.22: Comparison of experimental and theoretical vibration at mode 5 for damaged model

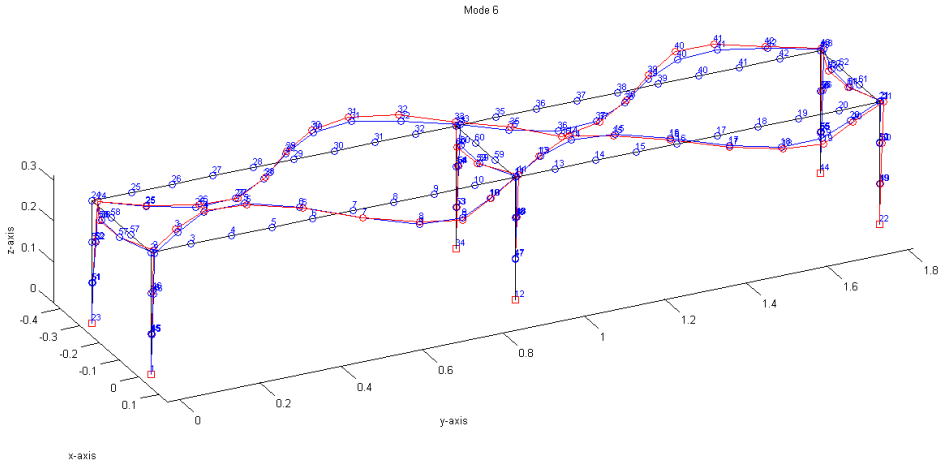

Figure 6.23: Comparison of experimental and theoretical vibration at mode 6 for damaged model

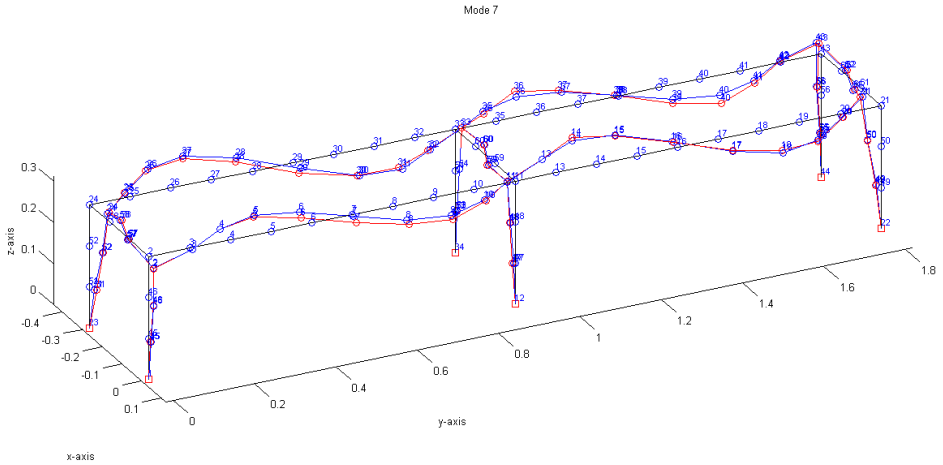

Figure 6.24: Comparison of experimental and theoretical vibration at mode 7 for damaged model

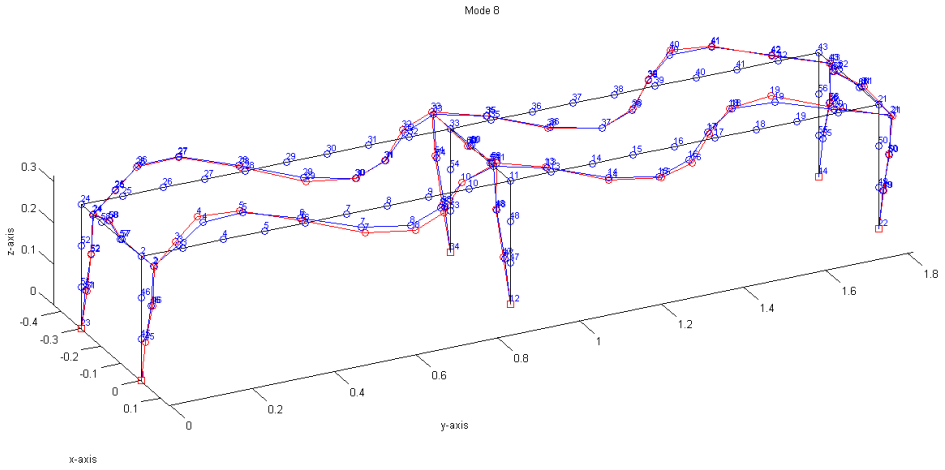

Figure 6.25: Comparison of experimental and theoretical vibration at mode 8 for damaged model

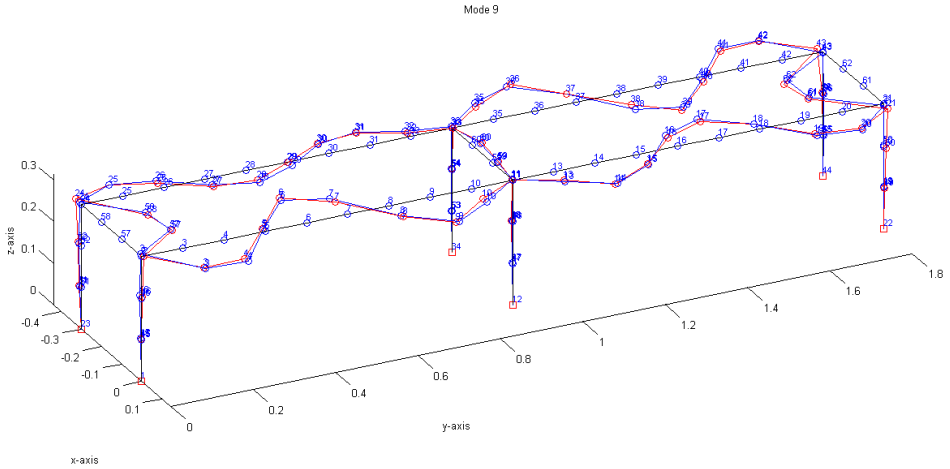

Figure 6.26: Comparison of experimental and theoretical vibration at mode 9 for damaged model

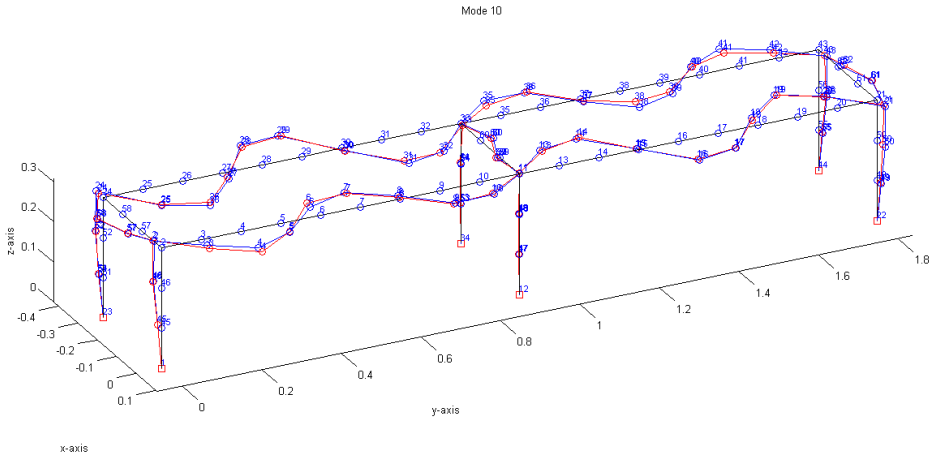

Figure 6.27: Comparison of experimental and theoretical vibration at mode 10 for damaged model

According to table 6.5, the Jv value and the corresponding updated parameters are shown, and the comparison is presented between undamaged and damaged conditions. The updated parameter K5 has the largest reduction in young's modulus, which is nearly four times larger than the second one. According to figure 6.15, the damage can be considered to be localized on longitudinal beam with updating parameter K5.

	Jv	K1	K2	K3	K4	K5	K6	K7	K8
Damaged	0.1878	0.7647	0.9604	0.8418	0.6979	0.8465	0.9514	0.9760	0.9617
Undamaged	0.1352	0.7631	0.9627	0.8243	0.6943	0.9297	0.9749	0.9490	0.9818
Error (%)	38.8847	0.2117	-0.2379	2.1317	0.5152	-8.9439	-2.4161	2.8409	-2.0488

Table 6.5: Comparison of updated parameters between undamaged and damaged model

After the rough damage localization, further optimization was carried out to localize the exact damage location. In this time, all the young's modulus is kept as constant except for the damaged beam. The damaged beam was

divided into three parts, and three updating parameters were assigned and showed in figure 6.28.

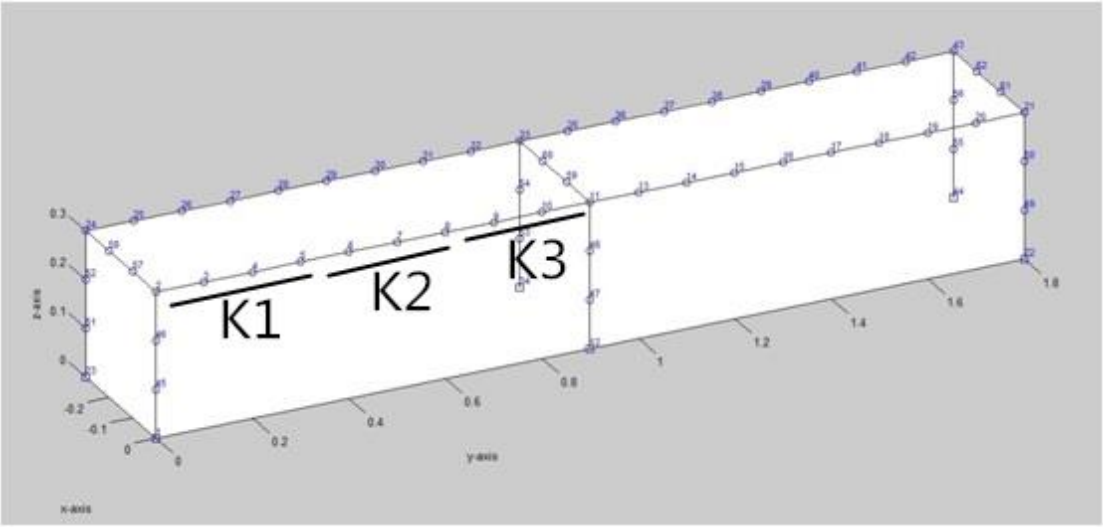

Figure 6.28: Assignment of updating parameters for further damage detection

According to table 6.6, the damage is obviously located at the element with K2 updating parameter in figure 6.28 which is exactly similar to the actual damage location. From table 6.7, figure 6.29 and figure 6.30, the frequencies and mode shapes are highly matched which can prove the reliability of the further damage detection. The vibration check is omitted as it is similar to the initial damage detection, and it would be tedious if it was presented again. As a result, only numerical comparisons were showed, and it is accurate enough.

The results are showed below:

	Jv	K1	K2	K3
Damaged	0.1947	0.940183	0.668506	0.96033
Undamaged	0.1352	0.9297	0.9297	0.9297
Error (%)	44.00888	1.130319	-28.0924	3.297469

Table 6.6: Comparison of updated parameters between undamaged and damaged

model

	Experiment (Hz)	Initial FE model (Hz)	Error (%)	MAC (%)
Mode 1	49.828	49.54124	-0.575498	99.604
Mode 2	59.28839	60.52184	2.080419	96.095
Mode 3	72.62213	72.32477	-0.409458	98.953
Mode 4	99.73562	99.00554	-0.732011	94.639
Mode 5	126.1123	125.1281	-0.780370	90.535
Mode 6	174.5207	174.4648	-0.032061	98.450
Mode 7	214.4781	210.9985	-1.622343	98.045
Mode 8	258.0243	254.0576	-1.537326	98.448
Mode 9	384.9567	382.3483	-0.677570	98.037
Mode 10	400.2313	394.8247	-1.350854	98.399

Table 6.7: Comparison of experimental and theoretical modal properties of damaged model in further damage detection

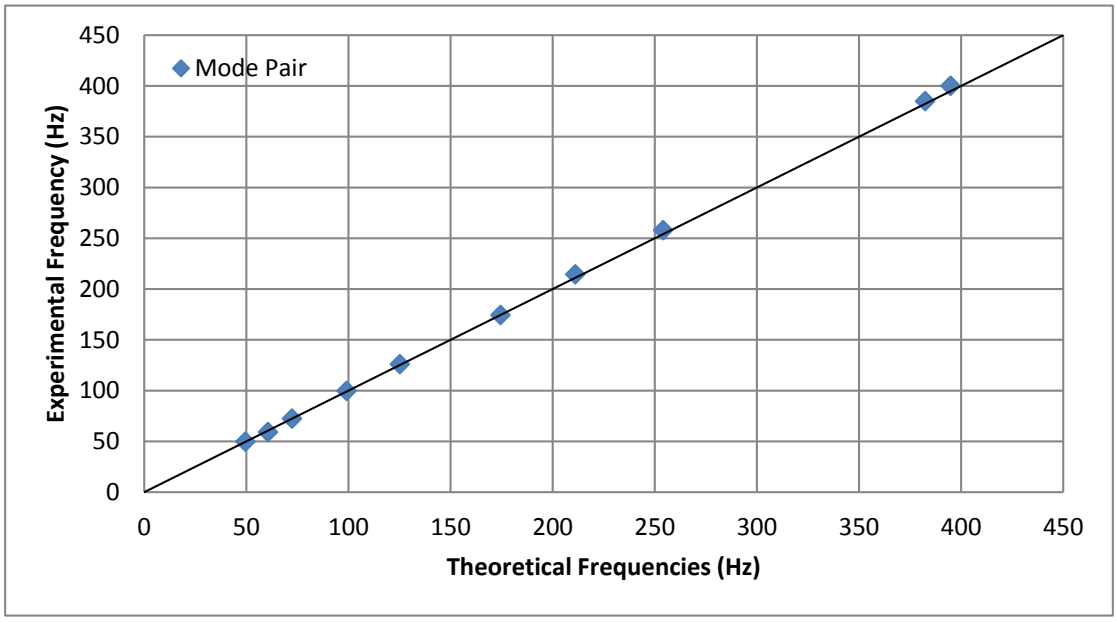

Figure 6.29: Frequency correlation of damaged model in further damage detection

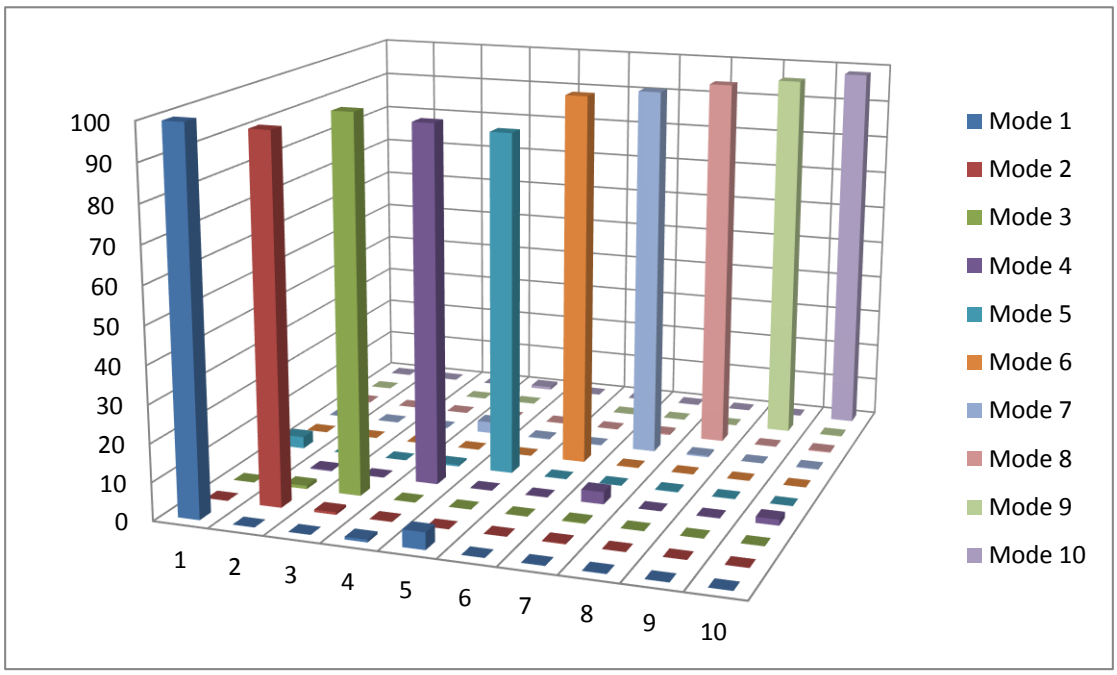

Figure 6.30: Mode shapes correlation of damaged model for further damage detection

6.4 Further Study - Frequency Residual Only

To study the damage detection by using frequency residual only, optimization was operated between undamaged and damaged stages. Eight updating parameters were used as shown in figure 6.1. According to the table 6.8, even though the Jv value is minimized a lot, but the corresponding updating parameters are totally unreasonable. The changes can determine the existence of damage, but it cannot provide any information for the location of damage. As a result, weighting factor cannot be too large in frequency residuals.

	Jv	K1	K2	K3	K4	K5	K6	K7	K8
Damaged	0.04	0.05	0.74	1.28	0.93	1.10	0.96	0.95	0.68
Undamaged	0.04	1.15	0.74	0.00	0.79	0.70	0.90	0.96	1.16
Error (%)	12.96	2371.27	-0.21	-99.89	-15.22	-36.82	-6.06	0.80	69.02

Table 6.8: Comparison of updated parameters when using frequency residuals only

6.5 Further Study – Discussion of Use of Optimization Method

For the optimization of damage detection in this case, it is not required to generate random trials of updating parameters. Instead, the updated parameters from undamaged model can be used for the initial trials. By studying, the final results are similar to the current example in Chapter 6.3. This method can save time in optimization. However, random inputs approach should still be used in the optimization of real infrastructure as there are too many uncertainties in huge and complex structures.

If random inputs approach was performed, it was suggested to set the maximum number of iterations allowed by using "optimset". By observation, the Jv value would start to converge after 40-50 iterations. Therefore, setting number of iterations and getting some minimum points for complete optimization is more efficient.

6.6 Chapter Conclusions

In this chapter, the damage is successfully detected and localized by using finite element model updating approach. A simulated finite element model was first built up, and the objective function, updating parameters, weighting factors and optimization algorithm were selected for damage detection.

It demonstrates that it is impossible to detect the location of damage when updating parameters are more than the considered modes. Besides, two-steps approach was used for damage localization without the loosing of accuracy, and the updating parameters can be controlled within a suitable and reasonable range. It also study the ability of damage localization by using frequency residuals only,

and the answer is it can only detect the existence of damage without providing any information about the damage location. Finally, the use of optimization algorithm is discussed to improve the time efficiency of damage detection.

CHAPTER 7: CONCLUSIONS

This thesis completely detects the existence and location of the damage in the scaled model accurately. Different kinds of useful techniques such as mode shape combining, mode shape normalization, modal assurance criterion and so on are demonstrated. In addition, the vibration measurement procedures are described generally, and the some recommendations are stated when it is applied on a real infrastructure. Furthermore, the analyzing methods and logic are presented clearly and commonly, so that it can be used in the real situation with only little modifications in the finite element model. The most important investigation is that using two-step optimization approach with less updating parameters is much better than using one-step optimization with more parameters. Two-step approach can detect the location of damage accurately and faster than the one step method as it reduces the number of updating parameters.

To be concluded, it is a feasible method that can be used in damage detection of overpasses in Hong Kong. It can significantly reduce the demand of human resources and provides accurate damage estimation rather than the visual inspection method.

References

1. Abdel Wahab, M., and De Roeck, G. (1999). “Damage detection in bridges using modal curvatures: Application to a real damage scenario” Journal of Sound and Vibration, 226(2), 217-235

2. Bernal, D., and Gunes, B. (2002). “Damage localization in output-only systems: a flexibility based approach.” Proceedings of the 20th Modal Analysis Conference, Los Angeles, 1185-1191.

3. Bernal, D., and Gunes, B. (2004). “Flexibility based approach for damage characterization: Benchmark application.” Journal of Engineering Mechanics, ASCE, 130(1), 61-70.

4. Cobb, R. G., and Liebst, B. S. (1997). “Structural damage identification using assigned partial eigenstructure.” AIAA Journal, p152(7).

5. Cobb, R. G., and Liebst, B. S. (1997). “Structural damage identification using assigned partial eigenstructure.” AIAA Journal, v35 n1 p152(7).

6. Cawley, P., Adams, R.D. (1979). “The locations of defects in structures from measurements of natural frequencies.” Journal of strain analysis, 14(2): 49-57.

7. Friswell, M.I., Penny, J.E.T., Wilson, D.A.L. (1994). “Using vibration data and statistical measures to locate damage in structures” Modal Analysis: The international journal of analytical and experimental modal analysis. 9(4): 239-254.

8. Ho, Y. K., and Ewins, D. J. (2000). “On structural damage identification with mode shapes” Proceedings of COST F3 Conference on System Identification and Structural Health Monitoring, Madrid, Spain, 677-686

9. Hou, Z., and Noori, M. (1999). “Application of wavelet analysis for structural health monitoring.” Proc., 2nd Int. Workshop on Struct. Health Monitoring, Stanford University, Stanford, Calif., 946-955

10. Huang, N. E.; Shen, Z.; Long, S. R.; Wu, M. C.; Shih, H. H.; Zheng, Q.; Yen, N. C.; Tung, C. C.; Liu, H. H. (1998). "The Empirical Mode Decomposition and the Hilbert Spectrum for Nonlinear and Nonstationary Time Series Analysis". Proceedings of the Royal Society of London 454 (1971): 903–995.

11. Idichandy, V.G., Ganapathy, C. (1990). "Modal parameters for structural integrity monitoring of fixed offshore platforms." Experimental Mechanics, 30(4): 382-391.

12. J.W.Cooley, J.W.Tukey.(1965) "An algorithm for the machine calculation of complex Fourier series", Math.Comp,1965,19(4):297-301.

13. Jaishi, B., and Ren, W. X. (2005). "Structural finite element model updating using ambient vibration test results." Journal of Structural Engineering, ASCE, 131(4), 617-628.

14. J. E. Mottershead, C. Mares, M. I. Friswell, and S. James. (2000) "Selection and updating of parameters for an aluminium space-frame model. Mechanical Systems and Signal Processing", 14(6), 923–944

15. Kaouk, M. and Zimmerman, D.C., (1992) "Structural Damage Detection Using a Minimum Rank Theory," Journal of Vibrations and Acoustics, Vol. 116, No.2, pp.222-231

16. Liu, P. L. (1995). "Identification and damage detection of trusses using modal data" J.Struct. Engrg., ASCE, Vol. 121, No. 599.

17. Mayes, R.L. (1992). "Error localization using mode shapes – An application to a two link robot arm." Proceedings of the 10th International Modal Analysis Conference – IMAC, 886-891.

18. M. I. Friswell and J. E. Mottershead.(1995) "Finite Element Model Updating in Structural Dynamics." Kluwer Academic Publishers, Dordrecht, Netherlands

19. Mottershead J. E., and Friswell M. I. (1993). "Model updating in structural dynamics: A Survey." Journal of Sound and Vibration, 167(2), 347-375.

20. Maeck, J., De Roeck, G. (2003). "Damage assessment using vibration analysis on the Z24-bridge." Mechanical systems and signal processing, 17 (1), 133-142

21. Nelson, R.B., (1976), "Simplified calculation of eigenvector derivatives." AIAA Journal, 14, pp. 1201-1205

22. P.W. Moller and O. Friberg. (1998), "Updating large finite element models in structural dynamics." AIAA Journal, 36(10), 1861-1868

23. Pandey, A. K., and Biswas, M. (1994). "Damage detection in structures using changes in flexibility." Journal of Sound and Vibration, 169 (1), 3-17.

24. Pandey, A. K., Biswas, M., and Samman, M. M. (1991). "Damage detection from changes in curvature mode shapes." Journal of Sound and Vibration, 145(2), 321-332.

25. R. J. Allemang and D.L. Brown. (1982) "A correlation for modal vector analysis". In Proceedings of IMAC I: 1st International Modal Analysis Conference, 110-116. 1982.

26. Scott W. Doebling, Charles R. Farrar, Michael B. Prime, Daniel W. Shevitz (1996). "Damage Identification and Health Monitoring of Structural and Mechanical Systems from Changes in Their Vibration Characteristics: A Literature Review." Report No. LA-13070-MS, Los Alamos National Laboratory Report, Los Alamos, New Mexico

27. Scott W. Doebling, Charles R. Farrar, Michael B. Prime, Daniel W. Shevitz (1998). "A Summary Review of Vibration-Based Damage Identification Methods" Shock and Vibration Digest

28. Sohn, H., Farrar, C. R., Hemez, F. M., Shunk, D. D., Stinemates, D. W., and Nadler, B. R.(2003). "A review of structural health monitoring literature: 1996-2001." Report No. LA-13976-MS, Los Alamos National Laboratory Report, Los Alamos, New Mexico

29. Stubbs, N., Osegueda, R. (1990a). “Global damage detection in solids-Experimental verification.” Modal analysis: The international journal of analytical and experimental modal analysis, 5(2): 81-97.

30. Stubbs, N. , Osegueda, R. (1990b). “Global non-destructive damage evaluation in solids.” Modal analysis: The international journal of analytical and experimental modal analysis, 5(2): 67-79.

31. Salawu, O.S. (1997). “Detection of structural damage through changes in frequency: A review.” Engineering Structures, 19(9): 718-723.

32. S.K. Au (2011), “Assembling mode shaped by least squares”, Mechanical Systems and Signal Processing, Volume 25, Issue 1, p. 163-179

33. Tshilidzi Marwala (2010), “Finite Element Model Updating Using Computational Intelligence Techniques: Applications to Structural Dynamics” Springer

34. Xu, Y. L., and Chen, J. (2004). “Structural damage detection using empirical mode decomposition: experimental investigation.” J. Engrg. Mech., ASCE, 130, 1279.

35. Xia, Y., Hao, H., Brownjohn, J. M. W., and Xia, P. Q. (2002). “Damage identification of structures with uncertain frequency and mode shape data.” Earthquake Engng Struct. Dyn., Vol. 31, 1053- 1066.

36. Y. L. Xu, and Y. Xia (2012). “Structural Health Monitoring of Long-Span Suspension Bridges” Spon Press, London and New York

37. Zhao, J., DeWolf, J. T. (1999). “Sensitivity study for vibration parameters used in damage detection.” Journal of Structural Engineering, ASCE, 125(4), 410-417.

Appendix

Appendix A

A.1 MATLAB code for extracting time domain data and transform to frequency domain data

```
clear;
clc;
ref=1; % Reference Channel
hit=1; % Number of hits
count=0;
count_set=zeros(hit,1); % number of impulses for each set of measurement.

filename={
    'st1_node6'
    }; %Data from Labview

for i=1:hit
    fname=filename{i};
    eval(['load ' fname '.lvm;']);
    eval(['[row,colm]=size(' fname ');']);
    eval(['time=' fname '(:,1);']);
    eval(['acc=' fname '(:,2:end-1);']);
    sensr_num=size(acc,2);
    dt=time(2)-time(1);

    for j=1:sensr_num
        acc(:,j)=acc(:,j)-mean(acc(:,j));
    end

    figure;
    plot(acc(:,1));
    title(fname);
    xlabel('Sample number');
    ylabel('Accerelation (m/s^2)');
    button=questdlg('Please click the starting and ending point!','Instruction','Yes');
```

```
    [myx1,myy1]=ginput(1);
    myx1=round(myx1);
    [myx2,myy2]=ginput(1);
    myx2=round(myx2);
    v = (myx1:myx2);

    if i==1
        L_respns=length(v);
    end

    vv=v(1):(v(1)+L_respns);
    count=count+1;
    count_set(i)=count_set(i)+1;
    respns(:,:,count) = acc(vv,:);
    clear vv;
    resample=1;
    acc=acc(1:resample:end,:);

    close;
    clear acc;
    clear v
    clear fname;
    clear time;
end

for m=1:count
  for k = 1:(sensr_num)
        [Sxy(:,k),XX(:,k),YY(:,k),ff(:,k)]=fft_cross(respns(:,k,m),respns(:,ref,m),dt);
  end
  avsptr_temp(:,m)=mean(abs(Sxy),2); % average spectrum.
  avfreq(:,m)=mean(ff,2);
  clear Sxy;
  clear XX;
  clear YY;
  clear ff;
end

avrg_spctr=mean(avsptr_temp,2);
```

```
avrg_freq=mean(avfreq,2);

figure;
semilogy(avrg_freq,avrg_spctr);
xlabel('Frequency (Hz)');
ylabel('Power spectral density (g^2/Hz)');
axis([30,500,0,1]);

ginput(10); % Get initial frequencies
Fr=ans(:,1);
save('st.mat','Fr','L_respns','count','dt','respns');
```

A.2 Prepare the input parameters for mode identification

```
clear;
clc;
load st.mat;
fs=51200/25; % sampling frequency.
time_point=0;

for i=1:L_respns
    TM(i)=time_point;
    time_point=time_point+dt;
end

pssbl_f=Fr;
fr_num=length(pssbl_f);

for s=1:count
    %the purpose of this "cc for-loop" is to divide the 72 possible
    %frequencies to 12 groups to analyze.

% Prepare the required data for modeid.
    in.ti = TM(1); % starting time
    in.tf = TM(L_respns); % ending time
    in.f = pssbl_f;% initial trial of natural frequencies in Hz
    in.z = ones(1,fr_num)./100; % length(Fr)=number of frequency entered
```

```
% initial trial of mode shapes
    in.modeshape = randn(size(respns,2),fr_num); % initial trial of mode shapes
    in.actout = 1:size(respns,2); % the channel number of the output responses in dto.x
    in.actmode = 1:fr_num; % the number of modes to be calculated
    in.title{1} = 'Column 1: x direction';
    dto.x = respns(:,:,s); % assign the measured data
    dto.ti = in.ti; % the starting time
    dto.dt = dt; % the time step
    dto.tf = in.tf; % the ending time
    dto.title{1} = 'Column 1: x direction'; % title again ... information only
    out=modeid(in,[],dto); % call modeid
    freqcy(:,s)=out.f;
    MSP(:,:,s)=out.modeshape;
    clear in;
    clear dto;
    clear out;

end
save('st1_mode.mat','freqcy','MSP');
```

A.3 MATLAB code for Combining of mode shapes

```
%assembling mode shapes using least square. (S.K. AU, 2011, "Assembling mode shapes by least
squares")

clear;
close all;
clc;
L{1}=[
    zeros(1,82)     1     zeros(1,35)%1, 45x
    zeros(1,83)     1     zeros(1,34)%2, 45y
    zeros(1,84)     1     zeros(1,33)%3   46x
    zeros(1,85)     1     zeros(1,32)%4   46y
    1                         zeros(1,117)%5   2x
    0                   1     zeros(1,116)%6   2y
    zeros(1,2)        1     zeros(1,115)%7   2z
    zeros(1,106)     1     zeros(1,11) %8   57y
    zeros(1,107)     1     zeros(1,10) %9   57z
```

```
    zeros(1,108)    1    zeros(1,9) %10 58y
    zeros(1,109)    1    zeros(1,8) %11 58z
    zeros(1,41)     1    zeros(1,76)%12 24x
    zeros(1,42)     1    zeros(1,75)%13 24y
    zeros(1,43)     1    zeros(1,74)%14 24z
    zeros(1,96)     1    zeros(1,21) %15 52x
    zeros(1,97)     1    zeros(1,20) %16 52y
    zeros(1,94)     1    zeros(1,23) %17 51x
    zeros(1,95)     1    zeros(1,22) %18 51y
    ];

L{2}=[
    zeros(1,3)      1    zeros(1,114)%1   3x
    zeros(1,4)      1    zeros(1,113)%2   3z
    zeros(1,5)      1    zeros(1,112)%3   4x
    zeros(1,6)      1    zeros(1,111)%4   4z
    1                    zeros(1,117)%5   2x
    zeros(1,1)      1    zeros(1,116)%6   2y
    zeros(1,2)      1    zeros(1,115)%7   2z
    zeros(1,7)      1    zeros(1,110)%8   5x
    zeros(1,8)      1    zeros(1,109)%9   5z
    zeros(1,108)    1    zeros(1,9)%10 58y
    zeros(1,109)    1    zeros(1,8)%11 58z
    zeros(1,44)     1    zeros(1,73)%12 25x
    zeros(1,45)     1    zeros(1,72)%13 25z
    zeros(1,46)     1    zeros(1,71)%14 26x
    zeros(1,47)     1    zeros(1,70)%15 26z
    zeros(1,48)     1    zeros(1,69)%16 27x
    zeros(1,49)     1    zeros(1,68)%17 27z
    ];

L{3}=[
    zeros(1,9)      1    zeros(1,108)%1   6x
    zeros(1,11)     1    zeros(1,106)%2   7x
    zeros(1,12)     1    zeros(1,105)%3   7z
    zeros(1,13)     1    zeros(1,104)%4   8x
    zeros(1,14)     1    zeros(1,103)%5   8z
    zeros(1,15)     1    zeros(1,102)%6   9x
```

```
    zeros(1,16)     1     zeros(1,101)%7    9z
    zeros(1,7)      1     zeros(1,110)%8    5x
    zeros(1,8)      1     zeros(1,109)%9    5z
    zeros(1,50)     1     zeros(1,67)%10 28x
    zeros(1,51)     1     zeros(1,66)%11 28z
    zeros(1,52)     1     zeros(1,65)%12 29x
    zeros(1,53)     1     zeros(1,64)%13 29z
    zeros(1,54)     1     zeros(1,63)%14 30x
    zeros(1,55)     1     zeros(1,62)%15 30z
    zeros(1,48)     1     zeros(1,69)%16 27x
    zeros(1,49)     1     zeros(1,68)%17 27z
    zeros(1,10)     1     zeros(1,107)%18 6z
    ];

L{4}=[
    zeros(1,17)     1     zeros(1,100)%1    10x
    zeros(1,18)     1     zeros(1,99)%2     10z
    zeros(1,19)     1     zeros(1,98)%3     11x
    zeros(1,20)     1     zeros(1,97)%4     11y
    zeros(1,21)     1     zeros(1,96)%5     11z
    zeros(1,15)     1     zeros(1,102)%6    9x
    zeros(1,16)     1     zeros(1,101)%7    9z
    zeros(1,88)     1     zeros(1,29)%8     48x
    zeros(1,89)     1     zeros(1,28)%9     48y
    zeros(1,56)     1     zeros(1,61)%10 31x
    zeros(1,57)     1     zeros(1,60)%11 31z
    zeros(1,58)     1     zeros(1,59)%12 32x
    zeros(1,59)     1     zeros(1,58)%13 32z
    zeros(1,54)     1     zeros(1,63)%14 30x
    zeros(1,55)     1     zeros(1,62)%15 30z
    zeros(1,60)     1     zeros(1,57)%16 33x
    zeros(1,61)     1     zeros(1,56)%17 33y
    zeros(1,62)     1     zeros(1,55)%18 33z
    ];

L{5}=[
    zeros(1,17)     1     zeros(1,100)%1    10x
    zeros(1,18)     1     zeros(1,99)%2     10z
```

```
    zeros(1,86)    1    zeros(1,31)%3    47x
    zeros(1,87)    1    zeros(1,30)%4    47y
    zeros(1,110)    1     zeros(1,7)%5    59y
    zeros(1,111)    1     zeros(1,6)%6    59z
    zeros(1,112)    1     zeros(1,5)%7    60y
    zeros(1,88)    1    zeros(1,29)%8    48x
    zeros(1,89)    1    zeros(1,28)%9    48y
    zeros(1,113)    1     zeros(1,4)%10   60z
    zeros(1,100)    1     zeros(1,17)%11   54x
    zeros(1,101)    1     zeros(1,16)%12   54y
    zeros(1,98)    1    zeros(1,19)%13   53x
    zeros(1,99)    1    zeros(1,18)%14   53y
    zeros(1,22)     1     zeros(1,95)%15 13x
    zeros(1,23)     1     zeros(1,94)%16 13z
    zeros(1,63)    1    zeros(1,54)%17 35x
    zeros(1,64)    1    zeros(1,53)%18 35z
    ];

L{6}=[
    zeros(1,24)     1     zeros(1,93)%1   14x
    zeros(1,25)     1     zeros(1,92)%2   14z
    zeros(1,26)     1     zeros(1,91)%3   15x
    zeros(1,27)     1     zeros(1,90)%4   15z
    zeros(1,110)    1     zeros(1,7)%5    59y
    zeros(1,111)    1     zeros(1,6)%6    59z
    zeros(1,28)     1     zeros(1,89)%7   16x
    zeros(1,88)    1    zeros(1,29)%8    48x
    zeros(1,89)    1    zeros(1,28)%9    48y
    zeros(1,29)     1     zeros(1,88)%10 16z
    zeros(1,65)    1    zeros(1,52)%11 36x
    zeros(1,66)    1    zeros(1,51)%12 36z
    zeros(1,67)    1    zeros(1,50)%13 37x
    zeros(1,68)    1    zeros(1,49)%14 37z
    zeros(1,22)     1     zeros(1,95)%15 13x
    zeros(1,23)     1     zeros(1,94)%16 13z
    zeros(1,69)    1    zeros(1,48)%17 38x
    zeros(1,70)    1    zeros(1,47)%18 38z
    ];
```

```
L{7}=[
    zeros(1,30)    1    zeros(1,87)%1    17x
    zeros(1,31)    1    zeros(1,86)%2    17z
    zeros(1,26)    1    zeros(1,91)%3    15x
    zeros(1,27)    1    zeros(1,90)%4    15z
    zeros(1,32)    1    zeros(1,85)%5    18x
    zeros(1,33)    1    zeros(1,84)%6    18z
    zeros(1,34)    1    zeros(1,83)%7    19x
    zeros(1,35)    1    zeros(1,82)%8    19z
    zeros(1,71)    1    zeros(1,46)%9    39x
    zeros(1,72)    1    zeros(1,45)%10 39z
    zeros(1,73)    1    zeros(1,44)%11 40x
    zeros(1,74)    1    zeros(1,43)%12 40z
    zeros(1,75)    1    zeros(1,42)%13 41x
    zeros(1,76)    1    zeros(1,41)%14 41z
    zeros(1,22)    1    zeros(1,95)%15 13x
    zeros(1,23)    1    zeros(1,94)%16 13z
    zeros(1,69)    1    zeros(1,48)%17 38x
    zeros(1,70)    1    zeros(1,47)%18 38z
    ];

L{8}=[
    zeros(1,36)    1    zeros(1,81)%1    20x
    zeros(1,37)    1    zeros(1,80)%2    20z
    zeros(1,38)    1    zeros(1,79)%3    21x
    zeros(1,39)    1    zeros(1,78)%4    21y
    zeros(1,40)    1    zeros(1,77)%5    21z
    zeros(1,77)    1    zeros(1,40)%6    42x
    zeros(1,34)    1    zeros(1,83)%7    19x
    zeros(1,35)    1    zeros(1,82)%8    19z
    zeros(1,78)    1    zeros(1,39)%9    42z
    zeros(1,79)    1    zeros(1,38)%10 43x
    zeros(1,80)    1    zeros(1,37)%11 43y
    zeros(1,81)    1    zeros(1,36)%12 43z
    zeros(1,75)    1    zeros(1,42)%13 41x
    zeros(1,76)    1    zeros(1,41)%14 41z
    zeros(1,114)   1    zeros(1,3)%15    61y
```

```
    zeros(1,115)    1    zeros(1,2)%16    61z
    zeros(1,116)    1    zeros(1,1)%17    62y
    zeros(1,117)    1                %18    62z
    ];

L{9}=[
    zeros(1,92)    1    zeros(1,25)%1    50x
    zeros(1,93)    1    zeros(1,24)%2    50y
    zeros(1,38)    1    zeros(1,79)%3    21x
    zeros(1,39)    1    zeros(1,78)%4    21y
    zeros(1,40)    1    zeros(1,77)%5    21z
    zeros(1,104)    1    zeros(1,13)%6    56x
    zeros(1,90)    1    zeros(1,27)%7    49x
    zeros(1,91)    1    zeros(1,26)%8    49y
    zeros(1,105)    1    zeros(1,12)%9    56y
    zeros(1,79)    1    zeros(1,38)%10 43x
    zeros(1,80)    1    zeros(1,37)%11 43y
    zeros(1,81)    1    zeros(1,36)%12 43z
    zeros(1,102)    1    zeros(1,15)%13    55x
    zeros(1,103)    1    zeros(1,14)%14    55y
    zeros(1,114)    1    zeros(1,3)%15    61y
    zeros(1,115)    1    zeros(1,2)%16    61z
    zeros(1,116)    1    zeros(1,1)%17    62y
    zeros(1,117)    1                %18    62z
    ];

FlNm=[
        'st1_mode_new.mat'
        'st2_mode_new.mat'
        'st3_mode_new.mat'
        'st4_mode_new.mat'
        'st5_mode_new.mat'
        'st6_mode_new.mat'
        'st7_mode_new.mat'
        'st8_mode_new.mat'
        'st9_mode_new.mat'
        ];
```

```
StpNum=size(FlNm,1);
MdNum=10; %how many mdoes considered
for ii=1:StpNum
    eval(['load ' FlNm(ii,:) ';']);
    MshpMsr{ii}=nrmlz(MSP);
    %n is the sensor number used in each setup.
    n(ii)=size(MshpMsr{ii},1);
    MSP=[];
    f(ii,:)=freqcy;
end
Fr=mean(f,1);



for mm=1:MdNum
A0=0;
for ii=1:StpNum
    I=eye(n(ii));
    A0=A0+L{ii}'*(I-MshpMsr{ii}(:,mm)*MshpMsr{ii}(:,mm)')*L{ii};
    I=[];
end
[Vctr,VluMtrx] = eig(A0);
[EVlu,Indx]=sort(diag(VluMtrx));
EVctr=Vctr(:,Indx);
MshpCmb0=nrmlz(EVctr(:,1));
Dof=size(MshpCmb0,1);
Flg=1;

while Flg>1e-6

  A=0;
  bb=0;
  for ii=1:StpNum
      Rnda(ii)=1-abs(MshpMsr{ii}(:,mm)'*(L{ii}*MshpCmb0))/norm(L{ii}*MshpCmb0);
      c(ii)=sgn(MshpMsr{ii}(:,mm),L{ii}*MshpCmb0)*norm(L{ii}*MshpCmb0);
      A=A+(1+Rnda(ii))*L{ii}'*L{ii};
      bb=bb+(-c(ii)*L{ii}'*MshpMsr{ii}(:,mm));
  end
  D=[
```

```
        A                bb*bb'
        eye(Dof)     A
        ];
    [Vctrc,VluMtrxc] = eig(D);
    [EVluc,Indxc]=sort(diag(VluMtrxc));
    EVctrc=Vctrc(:,Indxc);
    MshpCmb1=nrmlz(EVctrc(1:(end/2),1));
    Flg=1-mac(MshpCmb0,MshpCmb1,0);
    MshpCmb0=[];
    MshpCmb0=MshpCmb1;
    MshpCmb1=[];
    Vctrc=[];
    VluMtrxc=[];
    EVluc=[];
    Indxc=[];
    EVctrc=[];
    Rnda=[];
    c=[];
    D=[];
    disp('Flg=');
    disp(Flg);
end

MshpWhl(:,mm)=MshpCmb0;
Vctr=[];
VluMtrx=[];
EVlu=[];
Indx=[];
EVctr=[];
MshpCmb0=[];
end

save('MshpWhl.mat','MshpWhl');
save('Fr.mat','Fr');
```

Appendix B

B.1 Simulated Finite Element Model

```
clc;
% General information of bridge
B = 0.3; % Bay width
L = 0.9; % Span length
H = 0.3; % Story height
%The following are for columns.
bc = 0.5*0.0254; % Column's width
hc = 1.2*0.0254; % Column's sectional depth
Ac = bc*hc; %in m^2
Iyc = hc*(bc^3)/12; %in m^4
Izc = bc*(hc^3)/12; %in m^4
Ixc = Iyc+Izc; %in m^4
Ioc = Iyc+Izc; %in m^4
mc = 7800*Ac; %mass for per unit of length
%The following are for beams.
bb = 0.5*0.0254; % Beam's width
hb = 1.2*0.0254; % Beam's sectional depth
Ab = bb*hb; %in m^2
Iyb = hb*(bb^3)/12; %in m^4
Izb = bb*(hb^3)/12; %in m^4
Ixb = Iyb+Izb; %in m^4
Iob = Iyb+Izb; %in m^4
mb = 7800*Ab; %mass for per unit of length
G = 80e9; %in Pa
E = 210e9; %in Pa

% INput parameters:
%    node    = coordinates of nodes
%                 node(:,1) = x coordinate
%                 node(:,2) = y coordinate
%                 node(:,3) = z coordinate
%                 node(:,4) = x translation DOF index, 0 = restrained, 1 = free
%                 node(:,5) = y translation DOF index, 0 = restrained, 1 = free
%                 node(:,6) = z translation DOF index, 0 = restrained, 1 = free
```

```
%               node(:,7) = x rotation DOF index, 0 = restrained, 1 = free
%               node(:,8) = y rotation DOF index, 0 = restrained, 1 = free
%               node(:,9) = z rotation DOF index, 0 = restrained, 1 = free

%   point = point for locate the bending plane of elements
%               point(:,1) = x coordinate
%               point(:,2) = y coordinate
%               point(:,3) = z coordinate

%   elem    = element connectivity of the structure
%               elem(:,1) = starting node number
%               elem(:,2) = ending node number
%               elem(:,3) = element group number
%               elem(:,4) = connection flexibility at starting node
%               elem(:,5) = connection flexibility at ending node
%               4 & 5(set 0 for rigid connection)
%
%   prop    = proporty information for each element
%               prop(:,1) = A
%               prop(:,2) = Ix
%               prop(:,3) = Iy
%               prop(:,4) = Iz
%               prop(:,5) = Io
%               prop(:,6) = G    Shear modulus
%               prop(:,7) = E, Young's modules
%               prop(:,8) = m, mass per unit length

node = [
        0       0       0       0 0 0 0 0 0
        0       0       H        1 1 1 1 1 1
        0       L/9     H       1 1 1 1 1 1
        0       2*L/9   H       1 1 1 1 1 1
        0       3*L/9   H       1 1 1 1 1 1
        0       4*L/9   H       1 1 1 1 1 1
        0       5*L/9   H       1 1 1 1 1 1
        0       6*L/9   H       1 1 1 1 1 1
        0       7*L/9   H       1 1 1 1 1 1
        0       8*L/9   H       1 1 1 1 1 1
```

```
0       L       H       1 1 1 1 1 1
0       L       0       0 0 0 0 0 0
0       10*L/9  H       1 1 1 1 1 1
0       11*L/9  H       1 1 1 1 1 1
0       12*L/9  H       1 1 1 1 1 1
0       13*L/9  H       1 1 1 1 1 1
0       14*L/9  H       1 1 1 1 1 1
0       15*L/9  H       1 1 1 1 1 1
0       16*L/9  H       1 1 1 1 1 1
0       17*L/9  H       1 1 1 1 1 1
0       2*L     H       1 1 1 1 1 1
0       2*L     0       0 0 0 0 0 0
-B      0       0       0 0 0 0 0 0
-B      0       H       1 1 1 1 1 1
-B      L/9     H       1 1 1 1 1 1
-B      2*L/9   H       1 1 1 1 1 1
-B      3*L/9   H       1 1 1 1 1 1
-B      4*L/9   H       1 1 1 1 1 1
-B      5*L/9   H       1 1 1 1 1 1
-B      6*L/9   H       1 1 1 1 1 1
-B      7*L/9   H       1 1 1 1 1 1
-B      8*L/9   H       1 1 1 1 1 1
-B      L       H       1 1 1 1 1 1
-B      L       0       0 0 0 0 0 0
-B      10*L/9  H       1 1 1 1 1 1
-B      11*L/9  H       1 1 1 1 1 1
-B      12*L/9  H       1 1 1 1 1 1
-B      13*L/9  H       1 1 1 1 1 1
-B      14*L/9  H       1 1 1 1 1 1
-B      15*L/9  H       1 1 1 1 1 1
-B      16*L/9  H       1 1 1 1 1 1
-B      17*L/9  H       1 1 1 1 1 1
-B      2*L     H       1 1 1 1 1 1
-B      2*L     0       0 0 0 0 0 0
0       0       H/3     1 1 1 1 1 1
0       0       2*H/3   1 1 1 1 1 1
0       L       H/3     1 1 1 1 1 1
0       L       2*H/3   1 1 1 1 1 1
```

```
        0       2*L     H/3     1 1 1 1 1 1
        0       2*L     2*H/3 1 1 1 1 1 1
        -B      0       H/3     1 1 1 1 1 1
        -B      0       2*H/3 1 1 1 1 1 1
        -B      L       H/3     1 1 1 1 1 1
        -B      L       2*H/3 1 1 1 1 1 1
        -B      2*L     H/3     1 1 1 1 1 1
        -B      2*L     2*H/3 1 1 1 1 1 1
        -B/3    0       H       1 1 1 1 1 1
        -2*B/3 0        H       1 1 1 1 1 1
        -B/3    L       H       1 1 1 1 1 1
        -2*B/3 L        H       1 1 1 1 1 1
        -B/3    2*L     H       1 1 1 1 1 1
        -2*B/3 2*L      H       1 1 1 1 1 1
    ];

elem = [
    2   57 2 0 0
    57 58 2 0 0
    58 24 2 0 0
    11 59 2 0 0
    59 60 2 0 0
    60 33 2 0 0
    21 61 2 0 0
    61 62 2 0 0
    62 43 2 0 0
    2   3   2 0 0
    3   4   2 0 0
    4   5   2 0 0
    5   6   2 0 0
    6   7   2 0 0
    7   8   2 0 0
    8   9   2 0 0
    9   10 2 0 0
    10 11 2 0 0
    11 13 2 0 0
    13 14 2 0 0
    14 15 2 0 0
```

15 16 2 0 0
16 17 2 0 0
17 18 2 0 0
18 19 2 0 0
19 20 2 0 0
20 21 2 0 0
24 25 2 0 0
25 26 2 0 0
26 27 2 0 0
27 28 2 0 0
28 29 2 0 0
29 30 2 0 0
30 31 2 0 0
31 32 2 0 0
32 33 2 0 0
33 35 2 0 0
35 36 2 0 0
36 37 2 0 0
37 38 2 0 0
38 39 2 0 0
39 40 2 0 0
40 41 2 0 0
41 42 2 0 0
42 43 2 0 0
1 45 1 0 0
45 46 1 0 0
46 2 1 0 0
12 47 1 0 0
47 48 1 0 0
48 11 1 0 0
22 49 1 0 0
49 50 1 0 0
50 21 1 0 0
23 51 1 0 0
51 52 1 0 0
52 24 1 0 0
34 53 1 0 0
53 54 1 0 0

```
    54 33 1 0 0
    44 55 1 0 0
    55 56 1 0 0
    56 43 1 0 0
    ];

point = [
    -B      0       H+0.1 %make sure the starting node and ending node of beam
    -B      0       H+0.1
    -B      0       H+0.1
    -B      L       H+0.1
    -B      L       H+0.1
    -B      L       H+0.1
    -B      2*L     H+0.1
    -B      2*L     H+0.1
    -B      2*L     H+0.1
    0       L       H+0.1
    0       L       H+0.1
    0       L       H+0.1
    0       L       H+0.1
    0       L       H+0.1
    0       L       H+0.1
    0       L       H+0.1
    0       L       H+0.1
    0       L       H+0.1
    0       L       H+0.1
    0       2*L     H+0.1
    0       2*L     H+0.1
    0       2*L     H+0.1
    0       2*L     H+0.1
    0       2*L     H+0.1
    0       2*L     H+0.1
    0       2*L     H+0.1
    0       2*L     H+0.1
    0       2*L     H+0.1
    -B      L       H+0.1
    -B      L       H+0.1
    -B      L       H+0.1
    -B      L       H+0.1
```

```
    -B      L       H+0.1
    -B      L       H+0.1
    -B      L       H+0.1
    -B      L       H+0.1
    -B      L       H+0.1
    -B      2*L     H+0.1
    -B      2*L     H+0.1
    -B      2*L     H+0.1
    -B      2*L     H+0.1
    -B      2*L     H+0.1
    -B      2*L     H+0.1
    -B      2*L     H+0.1
    -B      2*L     H+0.1
    -B      2*L     H+0.1
    -B      2*L     H+0.1
    0       -L/2 H
    0       -L/2 H
    0       -L/2 H
    0       -L/2 H
    0       -L/2 H
    0       -L/2 H
    0       -L/2 H
    0       -L/2 H
    0       -L/2 H
    -B      -L/2 H
    -B      -L/2 H
    -B      -L/2 H
    -B      -L/2 H
    -B      -L/2 H
    -B      -L/2 H
    -B      -L/2 H
    -B      -L/2 H
    -B      -L/2 H
    ];

prop = [
    Ac    Ixc    Iyc    Izc    Ioc    G    E    mc
    Ab    Ixb    Iyb    Izb    Iob    G    E    mb
  ];
```

```
[Ks,K11,K21,K22,KE,TE,M11] = frame3d_modify(node,point,elem,prop);
[D,V]=eigen(K11,M11);
[wnumber,temp]=size(D);
Nf=D.^0.5./(2*pi);
```

Appendix C

C.1Mode shape Nomalization

```
%Normalize mode shapes by using Euclidean norm
function [Nmodeshape]=Nrmlz(modeshpe)
[No,MdNum]=size(modeshpe);
for i=1:MdNum
      L=norm(modeshpe(:,i));
      Nmodeshape(:,i)=modeshpe(:,i)./L;
end
```

C.2 Modal Assurance Criteria

```
% Modal Assurance Criteria (MAC)

%   m1, m2     =    modeshapes
%   type = 0, normal MAC calculation
%   type = 1, sign of vector may be neglective

function MAC=mac(m1,m2,type)
mm = m1'*m2;

mm1 = m1'*m1;
mm1 = diag(mm1);

mm2 = m2'*m2;
mm2 = diag(mm2);

if type==0                          %for normal MAC calculation
    MAC= mm.^2./(mm1*mm2');
```

```
else type==1                    %sign of input parameters should be considered
    MAC= mm./(mm1*mm2').^0.5;

end;
```

Appendix D

D.1 Objective function

```
%Objective function that minimize the difference of mode shapes.
function Jv = objfun_bridge(k)
global Fr MshpWhl MdNum Index Clc MAC;
[Nf,Mshp,K11,M11,node,elem,point,prop]=Bridge_with_coulmn_final(k);

%match the measured and calculated mode shapes using MAC.

[nodenum,temp]=size(node);

for ii=1:size(Mshp,1)
    Mshp_clc(:,ii)=Mshp(Index,ii); % Reduction of theoretical mode shape
end

Mshp_clc=nrmlz(Mshp_clc); %Normalization

%pair the modes using MAC.
MAC=mac(MshpWhl,Mshp_clc,0);
for ii=1:MdNum
    Clc(ii)=find(MAC(ii,:)==max(MAC(ii,:)));
end



%prepare the calculated mode shapes in different setups. check the sign of
%calculated and measured mode shapes in different segments of different setups.

for jj=1:MdNum
        if sgn(MshpWhl(:,jj),Mshp_clc(:,Clc(jj)))<0
            Mshp_clc(:,Clc(jj))=-Mshp_clc(:,Clc(jj));
```

```
        end
end



%objective function.
Jv=0;
        for kk=1:MdNum
            Jv=Jv+0.5*sqrt(((Fr(kk)-Nf(Clc(kk)))/Fr(kk))^2)+0.5*(1-MAC(kk,Clc(kk)));
        end
end
```

D.2 Optimization

```
%Optimization
clear all;
clc;
close all;
global Fr MshpWhl MdNum Index Clc MAC;
load MshpWhl.mat; %load measured mode shapes
load Fr.mat;          %load measured frequencies
load Index.mat;     %for reduction or expansion of model

MdNum=size(MshpWhl,2);
Mnm(1)=0; %min(1) is used to store the index of Vmin whose Jv is the smallest.
Mnm(2)=100e100; %min(2) is used to store the smallest Jv.

for p=1:1000 % set larger to achieve global minimum

    p
    k=0.001+(2.5-0.001).*rand(1,8); %Random trials

    option = optimset('Algorithm','active-set','Display','Iter');
    % Optimization
    [K,Jv]=fmincon('objfun_bridge',k,[],[],[],[],0.001.*ones(1,8),2.5.*ones(1,8),[],option);

    JJ(p)=Jv;
    Arrange(p,:)=Clc;
```

```
    if JJ(p)<Mnm(2)
        Mnm(1)=p;
        Mnm(2)=JJ(p);
        max_clc=Clc;
        max_MAC=MAC;
    end

    KK(p,:)=K;

    disp('Jmin=')
    disp(Mnm(2))
    disp('The temporary optimal coefficient vector is ')
    disp(KK(Mnm(1),:))

end
save('J.mat','JJ');
save('Clc.mat','Arrange');
save('KK.mat','KK');
save('Mnm.mat','Mnm');
save('mode.mat','max_MAC');
```